

# EXPLOITING NETWORK TOPOLOGY FOR LARGE-SCALE INFERENCE OF NONLINEAR REACTION MODELS

NIKHIL GALAGALI AND YOUSSEF MARZOUK

*Massachusetts Institute of Technology  
Cambridge MA, USA 02139*

**ABSTRACT.** The development of chemical reaction models aids system design and optimization, along with fundamental understanding, in areas including combustion, catalysis, electrochemistry, and biology. A systematic approach to building reaction network models uses available data not only to estimate unknown parameters, but also to learn the model structure. Bayesian inference provides a natural approach to this data-driven construction of models. Traditional Bayesian model inference methodology is based on evaluating a multidimensional integral for each model. This approach is often infeasible for nonlinear reaction network inference, as the number of plausible models can be combinatorially large. An alternative approach based on model-space sampling can enable large-scale network inference, but its efficient implementation presents many challenges. In this paper, we present new computational methods that make large-scale nonlinear network inference tractable. Firstly, we exploit the network-based interactions of species to design improved “between-model” proposals for Markov chain Monte Carlo (MCMC). We then introduce a sensitivity-based determination of move types which, when combined with the network-aware proposals, yields further sampling efficiency. These algorithms are tested on example problems with up to 1024 plausible models. We find that our new algorithms yield significant gains in sampling performance, thus providing a means for tractable inference over a large number reaction models with physics-based nonlinear species interactions.

## 1. INTRODUCTION

Detailed chemical reaction networks are a critical component of simulation tools in a wide range of applications, including combustion, catalysis, electrochemistry, and biology. In addition to being used as predictive tools, network models are also key to developing an improved understanding of the complex process under study. The development of reaction network models typically entails three tasks: selection of participating species, identification of species interactions (referred to as reactions), and the calibration of unknown parameter values. To this end, we are often faced with the challenge of comparing a combinatorially large number of reaction networks, while retaining physics-based reaction rate models. The ideas presented in this paper exploit the network-based interaction of species in reaction networks to make large-scale inference feasible. The notion of “sloppy models”—models in which the available data is able to tightly constrain only a few directions of the parameter space—is well

---

*E-mail address:* [nikhilg1@mit.edu](mailto:nikhilg1@mit.edu), [ymarz@mit.edu](mailto:ymarz@mit.edu).

*Key words and phrases.* reaction network | model selection | Bayesian inference | reversible-jump MCMC.

known in systems biology [12]. Our work exploits a similar sloppiness in the *structure* of reaction networks for big gains in the efficiency of network inference.

A standard approach to building models is to postulate reaction networks and to compare them based on their ability to reproduce indirect system-level experimental data. Data-driven approaches to network learning involve defining a metric of fit, e.g., penalized least-squares, cross-validation, model evidence, etc., and selecting models that optimize this metric. As such, the development of models involves not only the identification of the best model structure, but also the estimation of underlying parameter values given available data. Bayesian model inference provides a rigorous statistical framework for fusing data with prior knowledge to yield a full description of model and parameter uncertainties [7]. The application of Bayesian model inference to reaction networks, however, presents a significant computational challenge. Model discrimination in Bayesian analysis is based on computing model probabilities conditioned on available data, i.e., *posterior* model probabilities. Formally, the posterior model probability of a model  $M_n$  is given by

$$p(M_n|\mathcal{D}) = \frac{p(M_n)p(\mathcal{D}|M_n)}{\sum_n p(M_n)p(\mathcal{D}|M_n)},$$

where

$$p(\mathcal{D}|M_n) = \int \cdots \int p(\mathcal{D}|\mathbf{k}_n, M_n)p(\mathbf{k}_n|M_n)d\mathbf{k}_n$$

is known as the model evidence,  $p(M_n)$  is the prior probability of  $M_n$ ,  $\mathbf{k}_n$  is the parameter vector of model  $M_n$ , and  $\mathcal{D}$  refers to the available data. A common approach to Bayesian model inference is to assume linear/discrete model formulations and that the model parameters take conjugate priors, thereby making the calculation of individual model evidences analytically tractable. Reaction network inference has also been performed with linear/discrete modeling of species interactions and conjugate priors [5, 15]. In spite of the cheap analytical evaluation of evidence, the combinatorial explosion of the number of networks given species and their possible interactions precludes direct enumeration of model evidence. Thus, sampling based approaches have been developed for large-scale network inference in such contexts [4]. It is, however, widely believed that species interactions are more appropriately defined by the law of mass action. The law of mass action gives the rate of a chemical reaction (say  $X + Y \rightarrow Z$ ) as the product of a reaction-specific rate constant  $k$  with reactant concentrations  $[X]$  and  $[Y]$ :

$$(1.1) \quad \text{Rate} = -k[X][Y].$$

Using the law of mass action to define reaction rate produces a system of differential equations such that the parameters-to-observables map (*forward model*) is typically nonlinear. ODE-based species interaction models are now being incorporated into network inference frameworks [1, 16]. Rigorous computation of posterior model probabilities then requires evaluation of a high-dimensional integral for each model. A number of sampling-based methods exist in the literature for this purpose, but they are computationally taxing [3, 8]. When the number of competing models becomes large, the above methods actually become computationally *infeasible*.

Reaction network inference is particularly prone to this difficulty: instead of a few model hypotheses, one might start with a list of proposed reactions, for example, and form a collection of plausible models by considering all valid combinations of the proposed reactions. Alternative approaches such as Laplace's method and Bayesian

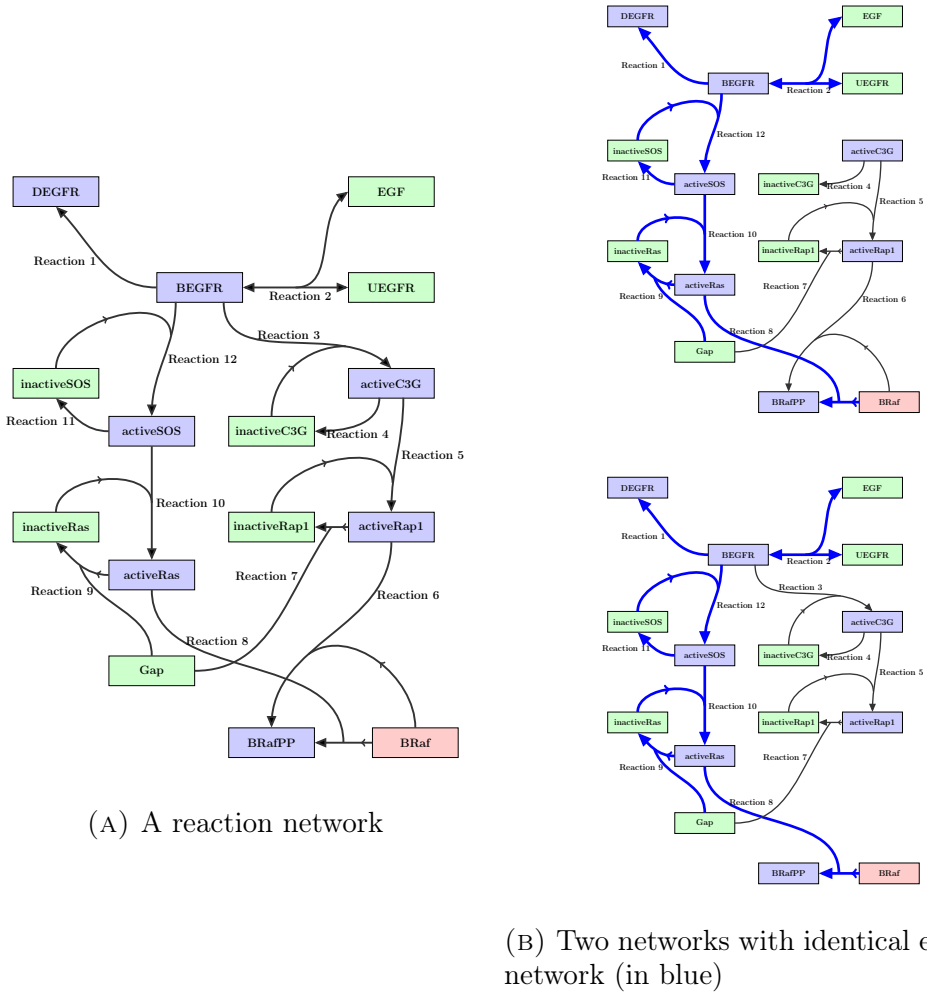


FIGURE 1. Chemical reaction networks

information criterion have been suggested, but they involve approximations of the posterior distribution. Across-model sampling offers a solution in cases where the number of models is large [10]. These methods work by making the sampler jump between models to explore the joint posterior distribution over models and parameters. Model probabilities are estimated from the number of times the sampler visits each model. The prohibitively high cost of model comparisons based on the computation of evidence for each model is avoided as the sampler visits each model in proportion to its posterior probability. Efficient across-model sampling, however, is challenging and requires a delicate design of proposals for between-model moves. Many practical applications of across-model sampling methods have relied on pilot posterior explorative runs to get a rough idea of the posterior distribution, although a few automated methods do exist in literature [10]. Large-scale network inference with nonlinear forward models has seen very limited work [6]. Oates et al. applied Bayesian model selection for the comparison of systematically generated models derived from ODE-based species interactions [14]. They used reversible-jump Markov chain Monte Carlo algorithm, a general across-model sampling method, for the simultaneous sampling of network topologies and their underlying parameters. The use of vanilla across-model sampling methods are generally known to perform poorly. There

is a need for the development of efficient large-scale network inference methods that would allow a systematic comparison of a large number of networks, but one that incorporates nonlinear forward models emerging from ODE-based species interaction formulations. In this paper, we present methods that exploit network topology of species interactions for efficient large-scale Bayesian inference of nonlinear chemical reaction networks.

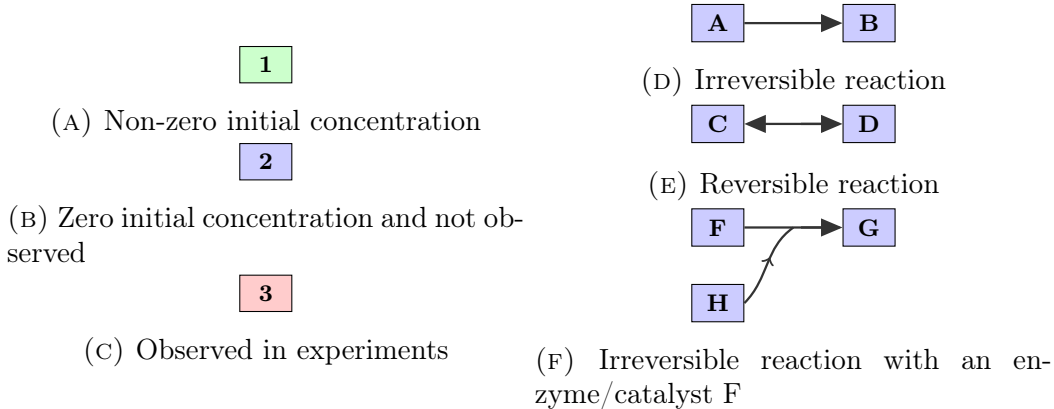


FIGURE 2. Taxonomy of reaction network elements

## 2. REACTION NETWORKS

**2.1. Reaction network elements.** A chemical reaction network generally consists of two different elements. Chemical species  $S$  and the interaction between species given by reactions  $R$ . Consider a simple reaction network shown schematically in Figure 14a. The reaction network consists of 15 nodes denoting the chemical species and 12 edges corresponding to reactions. We can classify all species into three categories (Figure 2). Species initially present (colored green) in the reaction system, species produced only during the operation (colored blue) of the system, and species that are either directly observed, or are directly linked to the observed data—referred to as *observables* (colored red). At the same time, there are commonly three types of reactions (Figure 2): irreversible reaction (single-headed arrow), reversible reaction (double-headed arrow), and irreversible/reversible reactions with enzymes (single-/double-headed arrows with pointers on branches connecting species that are consumed/produced). Enzymes are chemical species that are needed for the reaction to proceed, but do not get consumed or produced during the course of the reaction.

**2.2. Effective reaction network.** A reaction network may contain reactions that may not be active or reactions that are active and yet incapable of impacting the observables due to the network-based interactions of all species. Consider, for example, the two reaction networks shown in Figure 14b. We define the *effective network* of a reaction network to be the smallest subset of all reactions in the network that produces an identical value of the observables as the given reaction network. This implies that the reactions in addition to the effective network do not affect the observable value for any parameter setting, and the reaction network has the same marginal likelihood value as the effective reaction network. Both reduced networks shown in Figure 14b have the same effective network (Reactions 1, 2, 8, 9, 10, 11, 12). In reaction network 1, the non-production of species activeC3G renders reactions 4, 5, 6, and 7 inactive, and thus the value of the observable BRaf is independent of their

rate constant values. In case of reaction network 2, although reactions 3, 4, 5, and 7 are active, they are linked to the observable BRAF through species GAP and BEGFR, which are enzymes. Recall that catalyst/enzyme concentration is not affected by the reaction in which it participates. Thus, the observable is again independent of the rate constants of reactions 3, 4, 5, and 7.

**2.3. Determining effective networks from proposed reactions.** Before we begin sampling over the space of models and parameters, we first determine the effective networks of all plausible networks. If  $N$  is the total number of proposed reactions, the set of possible networks may be  $2^N$ , although incorporating prior knowledge to eliminate highly unlikely models may also be a practical choice. In either case, if the number of possible networks is very high, one may choose to determine effective networks online only for models visited by the sampler. Our procedure to determine the effective network given a set of reactions and observables is given by Algorithm 1 (Supplementary Information). The approach we employ to determine the effective network involves first identifying all reactions that are active given all species with nonzero initial concentration and then testing all active reactions to check if they actually influence the observables. The basis of the algorithm is an analysis of the topological structure of reaction networks, and does not require any ODE computation.

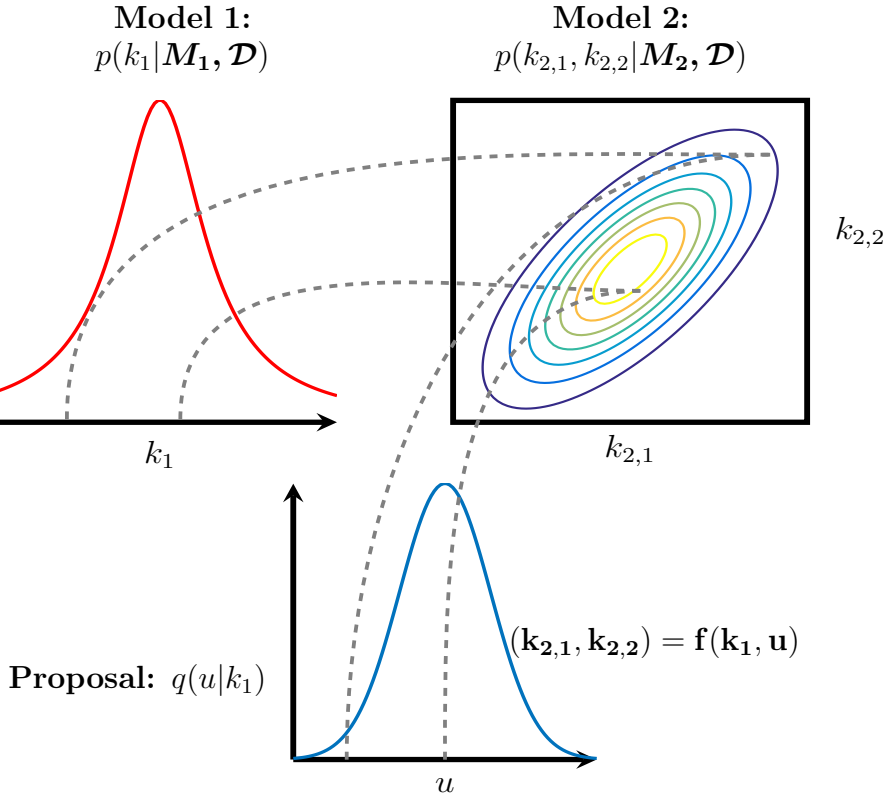


FIGURE 3. Efficient RJMCMC: align densities on  $(k_1, u)$  to  $(k_{2,1}, k_{2,2})$  accurately

### 3. REVERSIBLE JUMP MARKOV CHAIN MONTE CARLO

Reversible jump MCMC (RJMCMC) is a general framework to explore the posterior distribution over the joint space of models and parameters [11]. Consider the space of candidate models  $\mathcal{M} = \{M_1, M_2, \dots, M_N\}$ . Each model  $M_j$  has an  $n_j$ -dimensional vector of unknown parameters  $k_{M_j} \in \mathcal{R}_+^{n_j}$ , where  $n_j$  can take different values for different models. The RJMCMC algorithm simulates a Markov chain whose invariant distribution is the joint model-parameter posterior distribution  $p(M_j, k_{M_j} | \mathcal{D})$ . Each step of the algorithm consists of proposing a new vector of model-parameter values and accepting the proposed values according to an acceptance probability that also depends on the current model-parameter value vector. At any point of the state space, many different proposal moves can be constructed. Generally, the moves can be classified as between-model and within-model moves. The within model move involves using a standard Metropolis-Hastings proposal. A between-model move involves proposing a move to a different model and the corresponding set of parameter values. An irreducible and aperiodic transition kernel produces an ergodic reversible jump algorithm [11]. Further, ensuring that the posterior distribution over the models and parameters is the invariant distribution of the Markov chain is accomplished by satisfying the detailed balance condition. The detailed balance condition is enforced by constructing moves between any two models  $M$  and  $M'$  according to a bijective map  $f$  from  $(k_M, u)$  to  $(k_{M'}, u')$ , where  $u$  and  $u'$  known as dimension matching variables are such that  $\dim(k_{M'}) + \dim(u') = \dim(k_M) + \dim(u)$  and have densities  $q(u|k_M)$  and  $q(u'|k_{M'})$ , respectively. The choice of the distribution of  $u$  is part of the proposal construction and in addition to an appropriate  $f$  is key to an efficient RJMCMC simulation. At each step of the simulation, given the current state  $(M, k_M)$  a move to a new model  $M'$  is first proposed according to a chosen distribution  $q(M'|M)$ . Next, to move to  $(M', k_{M'})$  from  $(M, k_M)$  involves generating a sample of  $u$  according to  $q(u|k_M)$  and accepting the proposed move with probability  $\min\{1, A\}$ , where

$$(3.1) \quad A = \frac{p(M', \mathbf{k}_{M'} | \mathcal{D}) q(M|M') q(\mathbf{u}' | \mathbf{k}_{M'})}{p(M, \mathbf{k}_M | \mathcal{D}) q(M'|M) q(\mathbf{u} | \mathbf{k}_M)} |\det(\nabla f(\mathbf{k}_M, \mathbf{u}))|,$$

and  $(k_{M'}, u') = f(k_M, u)$ . The reverse move from  $(k_{M'}, u')$  to  $(k_M, u)$  is given by  $f^{-1}$  and has an acceptance probability  $\min\{1, A^{-1}\}$ . The model-move proposal  $q(M'|M)$  is generally chosen so that every move adds or delete one reaction. The selection of the jump function  $f$  and the parameter proposals  $q$  is based on the goal of improving between-model acceptances for both the forward ( $M \rightarrow M'$ ) and reverse ( $M' \rightarrow M$ ) model moves. Higher between-model acceptance rates may be obtained by “aligning” densities between the posterior and the proposals corresponding to the two models between which moves are proposed. As an example, consider moves between a one-dimensional model  $M_1$  ( $p(k_1 | \mathbf{M}_1, \mathcal{D})$ ) and a two-dimensional model  $M_2$  ( $p(k_{2,1}, k_{2,2} | \mathbf{M}_2, \mathcal{D})$ ) accomplished with proposal  $q(u|k_1)$  (Figure 3). By choosing the function  $f$  and the shape of the proposal  $q(u|k_1)$  such that the regions of high density and low density in the two spaces  $((k_1, u)$  and  $(k_{2,1}, k_{2,2})$ ) are mapping to each other (formally:  $p(k_1 | \mathbf{M}_1, \mathcal{D}) q(u|k_1) / \det(\nabla f(k_1, u))$  and  $p(f(k_1, u) | \mathbf{M}_2, \mathcal{D})$  have similar values) high between-model acceptance rates may be achieved. Intuitively, the above construction is attempting to choose  $f$  and  $q$  so as to make the acceptance rate close to 1 for all moves between the two spaces. For nested models, as is the case in the reaction network inference problem, a natural choice when proposing a move from a lower-dimensional model  $M$  to a higher dimensional model  $M'$  is to propose the

value of the rate constants of the newly added reactions according to  $q(\mathbf{u}|\mathbf{k}_M)$  and the values of the rate constants of reactions common to the two models fixed (henceforth  $1 : i$ ). Therefore,

$$(3.2) \quad \mathbf{f} := (\mathbf{k}_{M'}^{1:i}, \mathbf{k}_{M'}^{1:a}) = (\mathbf{k}_M^{1:i}, \mathbf{u}).$$

The reverse move in this case is deterministic. Let the proposal  $q(\mathbf{u}|\mathbf{k}_M)$  be given by

$$(3.3) \quad q(\mathbf{u}|\mathbf{k}_M) = \mathcal{N}(\mathbf{u}; \boldsymbol{\mu}, \boldsymbol{\Sigma}).$$

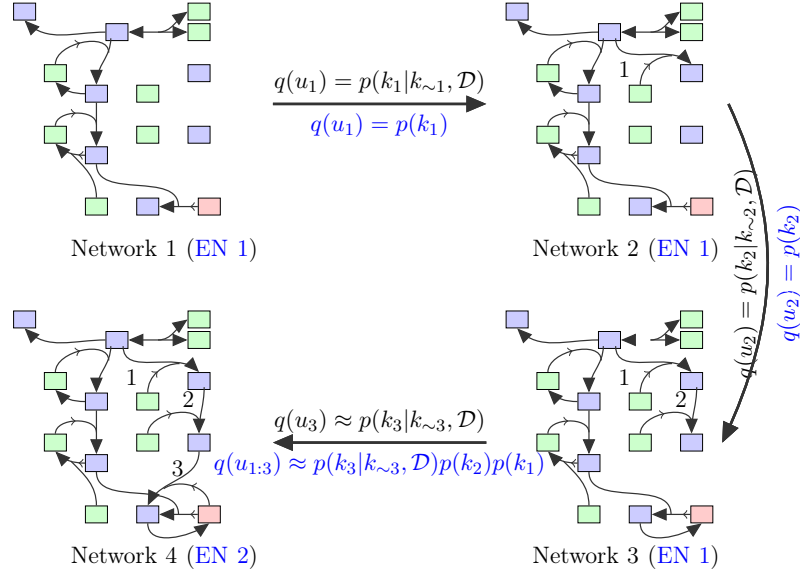
#### 4. NETWORK ANALYSIS FOR IMPROVED SAMPLING EFFICIENCY

**4.1. Network-aware parameter proposals.** The above proposal construction for between-model moves in which the parameter proposals adapt to conditional posterior densities produce efficient RJMCMC simulations [2, 9]. However, the direct application of the centered second-order conditions for between-model moves in the context of reaction network inference has a major drawback.

For example, consider a model-space sampler as shown in the top diagram of Figure 4. A standard model-space sampler adapts to the conditional posterior of the rate constant of the newly added reaction. The same model-space sampler when viewed in terms of the effective networks (network name and proposal shown in blue) shows that at each move of the sampler, if the move is between models with the same effective network, the proposal thus adapts to the prior distribution. Assuming that the prior distribution of each rate constant is independent Gaussian, the proposal matches the prior distribution for all rate constant values and the acceptance rate is identically equal to one for all moves. When the move is between two networks with different effective networks, the *effective proposal* is now the product of the prior distributions of all rate constants that did not produce a change in the effective network and the final effective-network-change producing reaction rate constant (See move between network 3 and effective network 2). Instead, we propose a network-aware (NA) approach, in which, because we have determined the effective networks, we design parameter proposals that adapt to the difference between the effective networks of the two networks. Thus, when the proposed move is between two networks with the same EN, we once again get the prior as the proposal distribution. However, when the proposed move is between two networks belonging to different ENs, we construct a proposal that approximates the conditional posterior distribution of the rate constants of all reactions *not included* in the two effective networks. As a result, at each step of the algorithm we obtain better alignment between the posterior and proposal densities and therefore superior sampling efficiency. A detailed description of the NA sampler along with the pseudocode of the steps involved are given in the Supplementary Information. To improve the chance of proposal acceptance one sets  $\boldsymbol{\mu}$  to be the posterior conditional mode. Next, one constructs an approximation to the posterior distribution by setting the covariance of the Gaussian to be the Hessian of the conditional posterior density. In other words, we construct a proposal which is a Gaussian approximation to the conditional posterior distribution  $p(\mathbf{k}_{M'}|\mathbf{k}_M, \mathcal{D})$ . In the framework of Brooks et al. [2], the above construction is equivalent to the centered second-order conditions.

**4.2. Sensitivity-based network-aware proposals.** In the context of reaction network inference, it is sometimes observed that a *maximum-a-posteriori* rate constant value for a reaction (\*) common to two networks differs substantially in the two networks. In such a case, keeping the rate constant of \* fixed when proposing moves

### Standard model space sampler



### Network-aware model space sampler

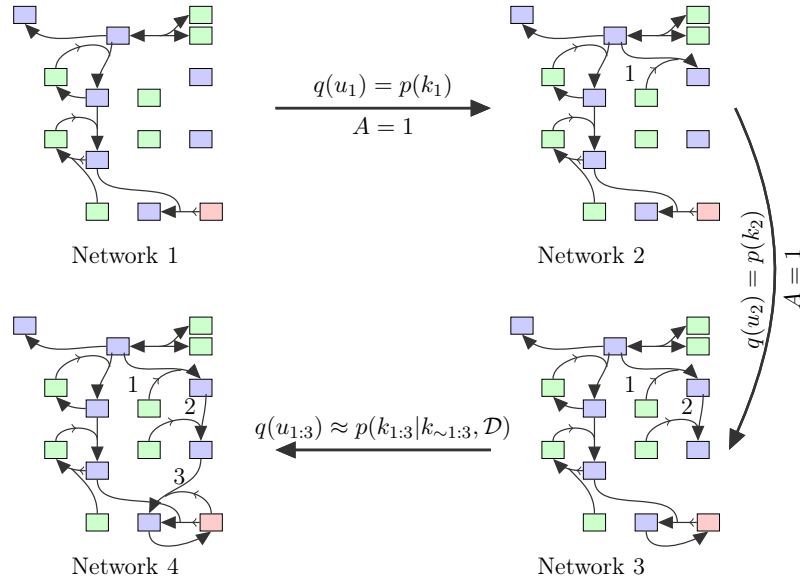


FIGURE 4. Model move from network 1 to 2 and 2 to 3 with network unaware (NUA) and network aware (NA) approaches leads to the proposal adapting to the prior. For the move between network 3 and 4, our NA approach proposes according to a proposal that approximates the joint conditional posterior  $p(k_1, k_2, k_3|k_{~1:3}, \mathcal{D})$ . In contrast the NUA approach retains the samples from the first two steps and constructs a proposal for the last move according to a proposal that approximates the conditional posterior  $p(k_3|k_{~3}, \mathcal{D})$

between the two networks leads to very poor acceptance rates. For instance, consider the example shown on the left in Figure 5, where the observable is highly sensitive to the value of  $k_1$ . As a result, the acceptance probability for moves which keep

the value of  $k_1$  fixed when proposing moves between Model 1 and Model 2 would produce very low acceptance rates. We propose a method to improve sampling efficiency of the network inference problem by identifying critical reactions common to the current and the proposed network and using a proposal distribution  $q$  for their rate constants in moves between the two networks. In other words, the reverse move from a high-dimensional effective network to a low-dimensional effective network is no longer deterministic. Figure 5 (right) shows pictorially how the aligning of densities is improved by including the high-sensitivity rate constant into proposal construction. When moves are proposed between Model 1 to Model 2 the values of rate constants  $k_1$  are proposed according to proposal distribution rather than keeping the values fixed. The proposal distribution  $q(u_{2,1}, u_{2,2})$  is designed to approximate the conditional posterior  $p(k_1, k_2 | M_2, k_{\{-1,2\}}, \mathcal{D})$  and the proposal  $q(u_{1,1})$  involved in the reverse move from Model 2 to Model 1 is designed to approximate the conditional posterior  $p(k_1 | M_1, k_{\{-1\}}, \mathcal{D})$ . The question we answer next is how one could identify “key” reactions whose inclusion in the proposal would improve MCMC mixing at a limited computational overhead. Given a set of observables and the current and proposed network, a useful strategy is to identify the reactions to which the posterior density is most sensitive. To determine the sensitivity of the posterior density to individual reactions given a network, we employ sensitivity analysis. Say, we have network  $M$  with reactions  $R_1, R_2, \dots, R_M$ . We determine the expected local sensitivity index  $\mathbb{E} \left[ \left| \frac{\partial \log p(k_i | \mathcal{D}, \mathbf{k}_{-i})}{\partial k_i} \right| \right]$  of reaction  $i$  with  $\mathbf{k}_{-i}^*$  given nominal values and the expectation taken with respect to the prior distribution  $p(k_i | M)$ . In practice, since the expectation is usually not analytically tractable, we settle for a noisy estimate of the expectation by evaluating the local sensitivity at a few realizations from the prior distribution and taking their average. Note similarity with the Morris method for global sensitivity analysis, except that we condition on nominal values of  $\mathbf{k}_{-i}^*$  [13]. Having determined the sensitivity of the log-posterior of the current and the proposed reaction network, we select a random number of high sensitivity reactions common to the two networks and include proposals for their rate constants in the forward and the reverse moves. The choice of the number of reactions to be included in the proposals is based on a Poisson distribution whose mean is kept at a small value. Choosing to include only a few common rate constant into the proposal is again based on the understanding that constructing effective proposals in high dimensions is generally hard. Thus, as the jump function for moves between models  $M$  and  $M'$  we have

$$(4.1) \quad \mathbf{f} := (\mathbf{k}_{M'}^{1:i}, \mathbf{k}_{M'}^{1:a}, \mathbf{k}_{M'}^{1:c}, \mathbf{u}'^{1:c}) = (\mathbf{k}_M^{1:i}, \mathbf{u}_M^{1:a}, \mathbf{u}^{1:c}, \mathbf{k}_M^{1:c}).$$

Here,  $\{1 : i\}$  are indices of reactions whose parameter values are kept fixed during moves between models  $M$  and  $M'$ ,  $\{1 : a\}$  are indices of reactions that are in model  $M'$  but not in  $M$ , and  $\{1 : c\}$  are reactions that are present in both models but whose rate constant values are determined according to respective proposal distributions. A detailed description of our sensitivity-based NA sampler is given in the Supplementary Information.

**4.3. Derandomization of conditional expectations.** The identification of *clusters* of models with identical EN can be further used for additional variance reduction. With the knowledge that all models in a cluster have identical model evidence, we can compute some expectations analytically and thereby obtain posterior averages of features with lower variances (SI).

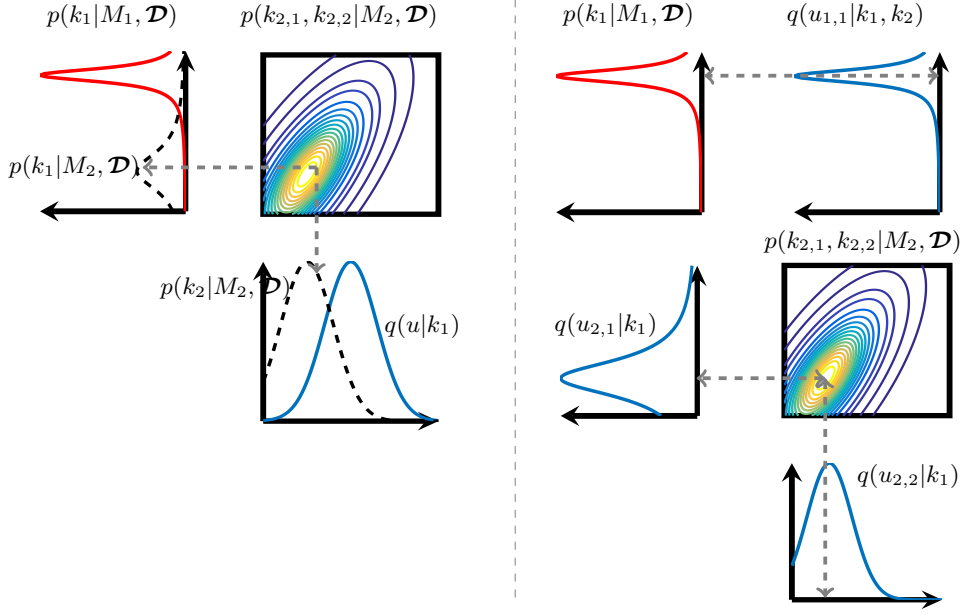


FIGURE 5. Sensitivity-based move determination (right) leads to densities being aligned; produces higher MCMC acceptance rates. Without sensitivity-based proposals (left), densities are unaligned.

## 5. MATERIALS

We present two example problems and demonstrate the efficiency of our NA sampling approaches compared to the NUA second-order approach of Brooks et al [2]. The examples we consider are a subset of reactions proposed for a protein-signalling network of the activation of extracellular signal-regulated kinase (ERK) by epidermal growth factor (EGF) [16]. The network diagram is shown in Figure 14a. The observable in our examples is the concentration of BRAF with the concentration evolution being modeled using the law of mass action/Michaelis-Menten functionals. The ODE forward model governing the evolution of species concentrations and the simulation methodology is described in detail in the Supplementary Information.

**5.1. Likelihood function.** The posterior probability in the Bayesian approach requires evaluating the likelihood function  $p(\mathcal{D}|\mathbf{k})$ , where  $\mathcal{D}$  are the data and  $\mathbf{k}$  are the reaction parameters. We employ an i.i.d. additive Gaussian model for the difference between model predictions and observations; thus the data are represented as

$$(5.1) \quad \mathcal{D} = \mathbf{G}(\mathbf{k}) + \boldsymbol{\epsilon}_n,$$

where  $\boldsymbol{\epsilon}_n \sim \mathcal{N}_n(\mathbf{0}, \sigma^2 \mathbf{I}_n)$ ,  $n$  is the number of observations,  $\mathbf{I}_n$  is an  $n$ -by- $n$  identity matrix, and  $\mathbf{G}(\mathbf{k})$  is the prediction of the forward model at the given value of the reaction parameters. The deterministic predictions  $\mathbf{G}(\mathbf{k})$  are obtained with the ODE integrator.

**5.2. Prior specification.** Since reaction rate constants must be positive, while their uncertainties may span multiple orders of magnitude, we take the prior distribution to be an independent log-normal distribution on each rate constant. That is,

$$(5.2) \quad p(k_i) : \log_{10} k_i \sim \mathcal{N}(\mu_{p,i}, \sigma_{p,i}^2).$$

The model prior distributions  $p(M)$  in the following examples are uniform.

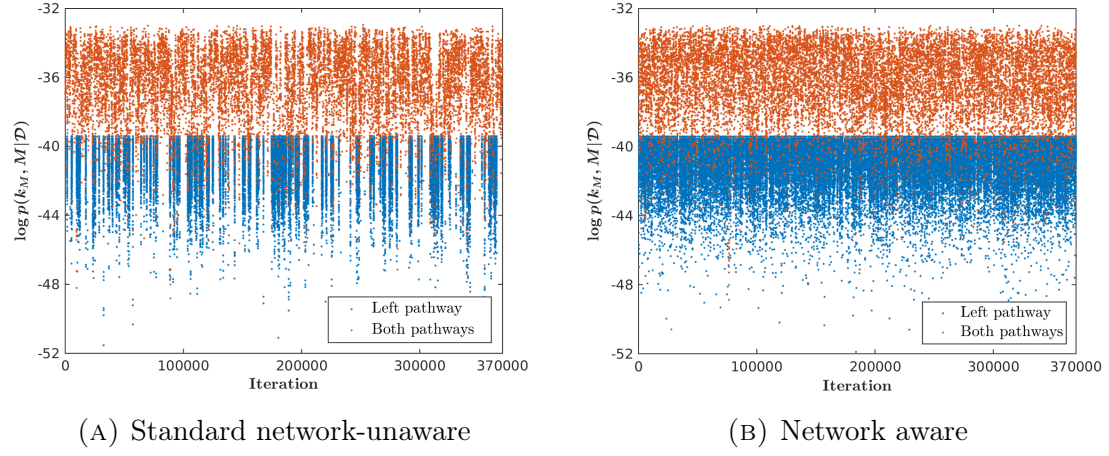


FIGURE 6. MCMC trace plots for Example 1

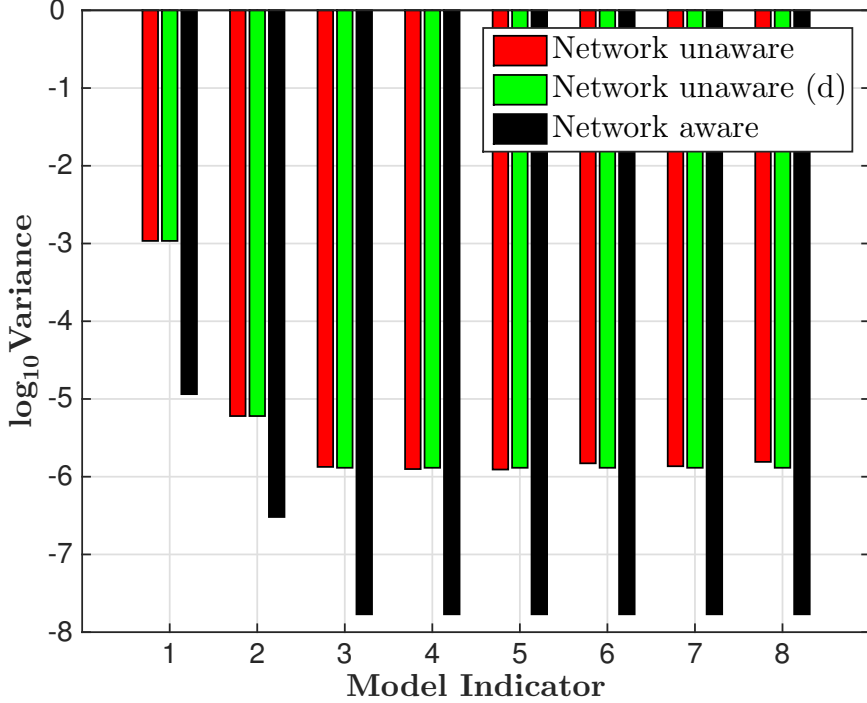


FIGURE 7. Variance comparison: NUA (with and without derandomization) and NA

## 6. RESULTS

**6.1. Example 1: five-dimensional nonlinear network inference.** In our first example, we keep reactions 1, 2, 8, 9, 10, 11, and 12 fixed and thus they are included in all the inferred models. The rate constants of all fixed reactions and Michaelis constants of all reactions are set to their base values (Supplementary Information). Reactions 3, 4, 5, 6, and 7 are taken to be uncertain. With the above five uncertain reactions, the number of potential models is 32. And with only BRAF as the observable, the number of ENs is 5. In this example, we compare our NA proposals to the

NUA approach. We generated 20 i.i.d. data points with noise model  $\mathcal{N}(0, 4)$  and rate constants and Michaelis constants set to their base values. The noise variance for the likelihood function, as in the data generating process, is taken as  $\sigma^2 = 4$ . We simulated 5 replications of 400000 samples using both the approaches. 30000 samples each were discarded as burn-in. The MCMC trace plots of the two approaches are shown in Figure 6. We see that frequency of moves between models operating with only the left pathway (blue samples) and both pathways (orange samples) is higher with our NA approach, thus indicating superior mixing. The performance of the two approaches is also evaluated by estimating the variance of model probability estimates. We find our NA approach produces model probability estimates whose variances are two orders-of-magnitude lower. A more useful comparison of the two schemes would be to compare the number of effective samples per unit time because it also incorporates the computational time. In the Supplementary Information, we present the effective sample size per minute values which confirms the favorability of our NA scheme.

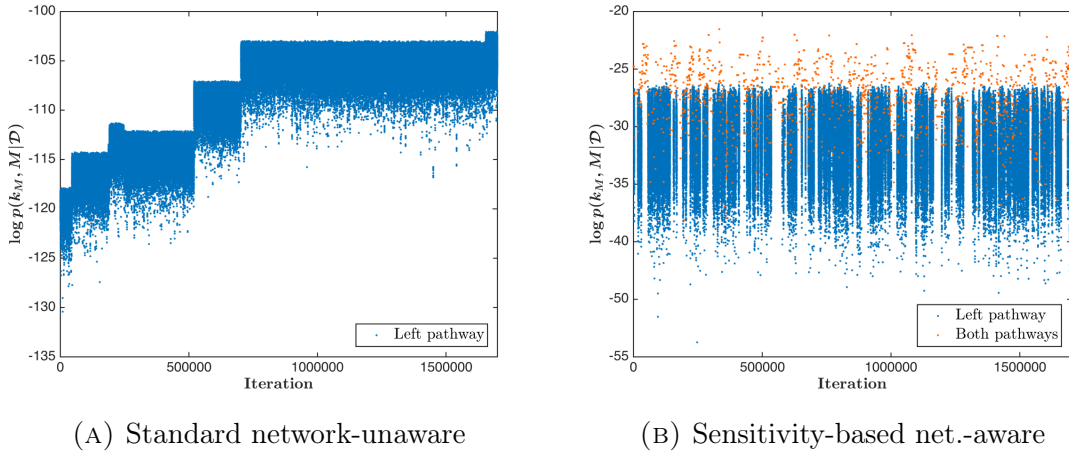


FIGURE 8. MCMC trace plots for Example 2

**6.2. Example 2: ten-dimensional nonlinear network inference.** In our second example, we keep only reactions 1 and 2 fixed. The rate constants of all fixed reactions and Michaelis constants of all reactions are set to their base values (Supplementary Information). Reactions 3–12 are uncertain, producing a total of 1024 potential models. And with only BRAF as the observable, the number of ENs is 24. In this example, we compare our sensitivity-based NA algorithm to the NUA approach of Brooks et al. We generated 30 i.i.d. data points with noise model  $\mathcal{N}(0, 0.04)$  and all rate constants and Michaelis constants set to their base values (Supplementary Information). The noise variance for the likelihood function, as in the data generating process, is taken as  $\sigma^2 = 0.04$ . We simulated 2 million samples using sensitivity-based NA approach and the NUA approach. 300,000 samples each were discarded as burn-in. The MCMC trace plots of the two approaches are shown in Figure 12. We see that the MCMC sampling of this 10-dimensional problem is in fact intractable using the standard approach: this can be seen by the inability of the sampler to switch between models belonging to left pathway and models that incorporate both pathways. In contrast our sensitivity-based NA sampler is able to move between the two pathways and efficiently explore the posterior distribution over all models and parameters. The

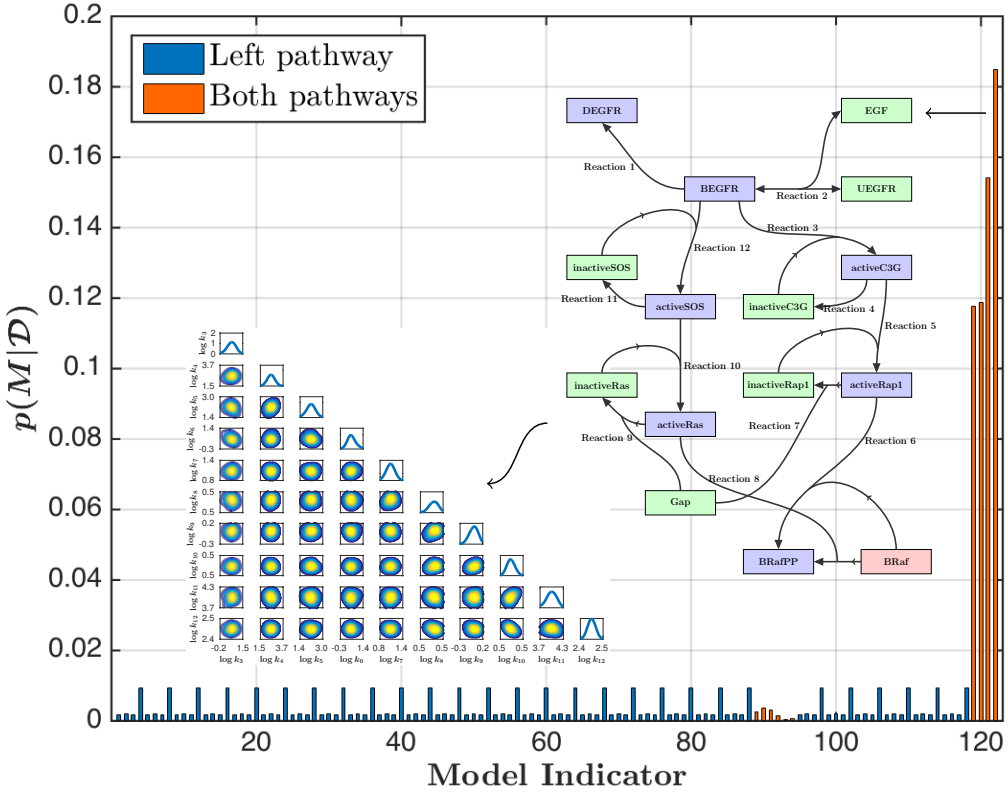


FIGURE 9. Above figure shows posterior probabilities of all models with non-zero probability, the network diagram of the model with the highest posterior probability, and the 1-dimensional and 2-dimensional marginal densities of the parameters of the highest-probability model in Example 2.

result is a sampler that allows large-scale inference of nonlinear reaction networks and provides myriad different information such as posterior probabilities of all models, parameter posterior densities, etc. (Figure 9)

## 7. CONCLUSIONS

Large-scale reaction network inference with differential equations based forward models is an important goal for improved fundamental understanding and better predictions in many areas. Systematic inference of reaction models that retains physics-based submodels, for example, by describing the reaction dynamics by mass action kinetics have hitherto been infeasible due to the very high computational cost involved. The algorithms presented in this paper exploit structural properties of reaction networks for efficient large-scale physics-based nonlinear network inference. Further development of network inference algorithms may be possible in the future by incorporating the NA approaches of this paper into across-model sampling methods that do not require mapping between parameter spaces.

## 8. ACKNOWLEDGMENTS

We acknowledge support from BP through the BP-MIT Energy Conversion Program.

## REFERENCES

- [1] K. Braman, T. A. Oliver, and V. Raman. Bayesian analysis of syngas chemistry models. *Combustion Theory and Modelling*, 17(5):858–887, 2013.
- [2] S. P. Brooks, P. Giudici, and G. O. Roberts. Efficient construction of reversible jump Markov chain Monte Carlo proposal distributions (with discussion). *Journal of Royal Statistical Society B*, 65:3–39, 2003.
- [3] S. Chib and I. Jeliazkov. Marginal likelihood from the Metropolis-Hastings output. *Journal of the American Statistical Association*, 96(453):270–281, 2001.
- [4] B. Ellis and W. H. Wong. Learning causal Bayesian network structures from experimental data. *Journal of the American Statistical Association*, 103(482):778–789, 2008.
- [5] N. Friedman, M. Linial, I. Nachman, and D. Pe’er. Using Bayesian networks to analyze expression data. *Journal of Computational Biology*, 7:601–620, 2000.
- [6] N. Galagali and Y. M. Marzouk. Bayesian inference of chemical kinetic models from proposed reactions. *Chemical Engineering Science*, 123:170–190, 2015.
- [7] A. Gelman, J. B. Carlin, H. S. Stern, and D. B. Rubin. *Bayesian Data Analysis*. Chapman and Hall/CRC, 2nd edition, 2004.
- [8] A. Gelman and X. L. Meng. Simulating normalizing constants: from importance sampling to bridge sampling to path sampling. *Statistical Science*, 13(2):163–185, 1998.
- [9] S. J. Godsill. On the relationship between Markov chain Monte Carlo methods for model uncertainty. *Journal of Computational and Graphical Statistics*, 10(2):230–248, 2001.
- [10] P. Green and D. Hastie. Reversible jump MCMC. Available at <http://www.maths.bris.ac.uk/~mapjg/papers/>. Access date: 04/24/2014, 2009.
- [11] P. J. Green. Reversible jump Markov chain Monte Carlo computation and model determination. *Annals of Stat*, 82(4):711–732, 1995.
- [12] R. N. Gutenkunst, J. J. Waterfall, F. P. Casey, K. S. Brown, C. R. Myers, and J. P. Sethna. Universally sloppy parameter sensitivities in systems biology models. *PLoS Computational Biology*, 3(10):e189, 2007.
- [13] M. D. Morris. *Technometrics*, (33):161–174, 1991.
- [14] C. J. Oates, B. T. Hennessy, Y. Lu, G. B. Mills, and S. Mukherjee. Network inference using steady-state data and Goldbeter-Koshland kinetics. *Bioinformatics*, 28(18):2342–2348, 2012.
- [15] K. Sachs, D. Gifford, T. Jaakkola, P. Sorger, and D. A. Lauffenburger. Bayesian network approach to cell signaling pathway modeling. *Science STKE*, 148:pe38, 2002.
- [16] T.-R. Xu, V. Vyshevsky, A. Gormand, A. von Kriegsheim, M. Girolami, G. S. Baillie, D. Kettley, A. J. Dunlop, G. Milligan, M. D. Houslay, and W. Kolch. Inferring signaling pathway topologies from multiple perturbation measurements of specific biochemical species. *Science Signaling*, 3(113):ra20, 2010.

## SUPPLEMENTARY INFORMATION

## 9. EFFECTIVE NETWORKS

**9.1. Determining effective networks from proposed reactions.** Recall that we defined the effective network of a reaction network to be the smallest subset of all reactions in the network that produces an identical value of the observables as the given reaction network. This implies that the reactions in addition to the effective network do not affect the observable value for any parameter setting, and the reaction network has the same marginal likelihood value as the effective reaction network. Before we begin sampling over the space of models and parameters, we first determine the effective networks of all plausible networks. If  $N$  is the total number of

proposed reactions, the set of possible networks may be  $2^N$ , although incorporating prior knowledge to eliminate highly unlikely models may also be a practical choice. In either case, if the number of possible networks is very high, one may choose to determine the effective networks online only for models visited by the sampler. Our procedure to determine the effective network given a set of reactions and observables is given by Algorithm 1. The approach we employ to determine the effective network involves first identifying all reactions that are active given all species with nonzero initial concentration and then testing all active reactions to check if they actually influence the observables. The steps involved in checking whether a particular active reaction influences the observables are given by Algorithm 2.

**9.2. The space of model clusters.** Given a set of proposed reactions, we can determine the effective reaction networks for all reaction networks using the algorithm in the last section. We are now in a position to define *clusters of models*. A cluster is defined as the collection of all models with the same effective network. Thus, assuming the models have been assigned a prior distribution  $p(M)$ , the cluster prior probability is given by

$$(9.1) \quad p(C_K) = \sum_{M_m \in C_K} p(M_m).$$

Further, the set of clusters has the following property:

$$(9.2) \quad C_K \cap C_J = \emptyset \text{ for } K \neq J$$

and

$$(9.3) \quad \bigcup_K C_K = \mathcal{M},$$

where  $\mathcal{M}$  is the complete space of all networks.

## 10. REVERSIBLE JUMP MARKOV CHAIN MONTE CARLO

We described the reversible jump MCMC algorithm in the paper. As discussed, the selection of a good map  $\mathbf{f}$  and the design of proposal distribution  $q(\mathbf{u}|\mathbf{k}_M)$  in RJMCMC is challenging and often chosen based on pilot simulations. The high cost and typically poor performance of the pilot-run based RJMCMC has prompted the development of methods for automatic proposal construction [1, 2, 3, 4, 6, 7]. All the above methods attempt to increase the acceptance rate of between-model moves at an additional computational expense, and have shown to improve performance in a number of cases. Brooks et al. [2] provide a general framework to understand and construct efficient reversible-jump proposals based on an analysis of the acceptance probability. Our work fits in their  $n^{th}$ -order condition proposal framework and we briefly review it here.

**10.0.1. Centered  $n^{th}$ -order condition based proposals.** The  $n^{th}$ -order ( $n \geq 1$ ) proposal conditions of Brooks et al. [2] is based on setting a series of derivatives (with respect to  $\mathbf{u}$ ) of the acceptance ratio  $A$  for proposal moves between models  $M$  and  $M'$  to the zero vector at a specific point  $\mathbf{c}_{M \rightarrow M'}(\mathbf{k}_M)$  known as the *centering point*:

**Algorithm 1** Effective reaction network from a set of reactions

---

```

1: Given:  $\mathbf{R}_{prop}$ : proposed reactions;  $\mathbf{S}_{in}$  species initially present;
2:  $\mathbf{R}_e$ : reactions in effective network,  $\mathbf{R}_e = \emptyset$ ;  $\mathbf{S}_e$ : species in the effective network,
    $\mathbf{S}_e = \mathbf{S}_{in}$ 
3:  $\mathbf{r}_i$ : reactants of reaction  $i$ ;  $\mathbf{p}_i$ : products of reaction  $i$ ;  $\mathbf{a}_i$ : enzymes of reaction  $i$ 
4:  $n'_e = 0$ ,  $t'_e = 0$ 
5: while  $n'_e \neq |\mathbf{R}_e|$  and  $t'_e \neq |\mathbf{S}_e|$  do
6:    $n'_e = |\mathbf{R}_e|$  and  $t'_e = |\mathbf{S}_e|$ 
7:   for  $i = 1$  to  $|\mathbf{R}_{prop}|$  do
8:     if Reaction  $R_i$  irreversible then
9:       if  $(\mathbf{r}_i \cup \mathbf{a}_i) \in \mathbf{S}_e$  then
10:         $\mathbf{R}_e = \mathbf{R}_e \cup R_i$  and  $\mathbf{S}_e = \mathbf{S}_e \cup \mathbf{p}_i$ 
11:     else if Reaction  $R_i$  is reversible then
12:       if  $(\mathbf{r}_i \cup \mathbf{a}_i) \in \mathbf{S}_e$  or  $(\mathbf{p}_i \cup \mathbf{a}_i) \in \mathbf{S}_e$  then
13:          $\mathbf{R}_e = \mathbf{R}_e \cup R_i$  and  $\mathbf{S}_e = \mathbf{S}_e \cup \mathbf{p}_i \cup \mathbf{r}_i$ 
14:    $\mathbf{R}_{active} = \mathbf{R}_e$ 
15:   for  $i = 1$  to  $|\mathbf{R}_e|$  do
16:     Inf  $\leftarrow$  Algorithm 2 ( $\mathbf{R}_{active}$ ,  $R_i$ )
17:     if Inf==0 then
18:        $\mathbf{R}_e = \mathbf{R}_e \setminus \{R_i\}$ 

```

---

**Algorithm 2** Algorithm to check if reaction  $R_I$  influences the observables

---

```

1: Given: Active reactions  $\mathbf{R}_{act}$ ; Observables  $\mathbf{O}$ 
2:  $\mathbf{S}_{inc}$ : collection of species,  $\mathbf{S}_{inc} = \mathbf{r}_i \cup \mathbf{p}_i$ ;  $\mathbf{R}_{inc}$ : collection of reactions,  $\mathbf{R}_{inc} = R_i$ 
3:  $t'_{inc} = 0$ 
4: while  $t'_{inc} \neq |\mathbf{S}_{inc}|$  do
5:    $t'_{inc} = |\mathbf{S}_{inc}|$ 
6:   for  $j = 1$  to  $|\mathbf{R}_{act}|$  do
7:     if  $R_j \notin \mathbf{R}_{inc}$  then
8:       if  $\mathbf{r}_j \cup \mathbf{a}_j \in \mathbf{S}_{inc}$  or  $\mathbf{p}_j \in \mathbf{S}_{inc}$  then
9:          $\mathbf{R}_{inc} = \mathbf{R}_{inc} \cup R_j$ 
10:    for  $j = 1$  to  $|\mathbf{R}_{inc}|$  do
11:       $\mathbf{S}_{inc} = \mathbf{S}_{inc} \cup \mathbf{p}_j \cup \mathbf{r}_j$ 
12: if  $\mathbf{O} \in \mathbf{S}_{inc}$  then
13:   Inf=1

```

---

$$(10.1) \quad \nabla^n A[(M, \mathbf{k}_M), (M', \mathbf{c}_{M \rightarrow M'}(\mathbf{k}_M))] = \mathbf{0}$$

The centering point  $\mathbf{c}_{M \rightarrow M'}(\mathbf{k}_M)$  is taken to be the equivalent point of parameter vector  $\mathbf{k}_M$  in model  $M'$ . Centering the proposal  $q(\mathbf{u} | \mathbf{k}_M)$  at the conditional maximum of the posterior density  $p(\mathbf{f}(\mathbf{k}_M, \mathbf{u}), M')$  is one intuitive choice and aims to increase the frequency of moves between models. In addition to the  $n^{th}$ -order condition, Brooks et al. [2] also introduce the zeroth-order condition in which the acceptance ratio is set to 1 at the centering point. Note the traditional random-walk Metropolis algorithm for posterior distribution on  $\mathbb{R}^m$  satisfies the zeroth-order condition at a central move corresponding to a step of size  $\mathbf{0}$ . Similarly, Langevin algorithms satisfy

both the zeroth-order and first-order conditions at the above central move. The zeroth and  $n^{th}$  order conditions aim to adapt proposal parameters on the current state of the chain  $(M, \mathbf{k}_M)$ , instead of relying on constant proposal parameters for all state transitions. Brooks et al. [2] further show that for a simple two model case, choosing the conditional posterior distribution of the parameters as the proposal distribution is optimal in terms of the capacitance of the algorithm. The  $n^{th}$ -order conditions attempt to achieve this goal by setting the derivatives of the acceptance ratio to be zero [9].

## 11. NETWORK ANALYSIS FOR IMPROVED SAMPLING EFFICIENCY

**11.1. Constructing parameter proposals.** In the paper, we described the network-unaware second-order approach of Brooks et al. [2] that attempts to approximate the conditional posterior by a Gaussian distribution. We provide further details here. For nested models, as is the case in the reaction network inference problem, a natural choice of the jump function  $\mathbf{f}$  is to choose the identity function. Thus, when proposing a move from a lower-dimensional model  $M$  to a higher dimensional model  $M'$ , the rate constants of the newly added reactions is proposed according to  $q(\mathbf{u}|\mathbf{k}_M)$  and the values of the rate constants of reactions common to the two models are kept fixed (henceforth  $1 : i$ ). Therefore,

$$(11.1) \quad \mathbf{f} := (\mathbf{k}_{M'}^{1:i}, \mathbf{k}_{M'}^{1:a}) = (\mathbf{k}_M^{1:i}, \mathbf{u}_M^{1:a}).$$

and the acceptance probability is given by

$$(11.2) \quad \alpha(\mathbf{k}_M, \mathbf{k}_{M'}) = \min \left\{ 1, \frac{p(M', \mathbf{k}_{M'}|\mathcal{D})q(M|M')}{p(M, \mathbf{k}_M|\mathcal{D})q(M'|M)q(\mathbf{u}|\mathbf{k}_M)} \right\}.$$

The reverse move in this case is deterministic. Let the proposal  $q(\mathbf{u}|\mathbf{k}_M)$  be given by

$$(11.3) \quad q(\mathbf{u}|\mathbf{k}_M) = \mathcal{N}(\mathbf{u}; \boldsymbol{\mu}, \boldsymbol{\Sigma}).$$

To improve the chance of proposal acceptance we center the proposal distribution at the conditional mode of the posterior distribution. Next, we construct an approximation to the posterior distribution by setting the covariance of the Gaussian to be the Hessian of the conditional posterior density. In other words, we construct a Gaussian approximation to the conditional posterior distribution. In the framework of Brooks et al., the above construction is equivalent to the centered second-order conditions. In the scheme described above, the mean vector  $\boldsymbol{\mu}$  is set to the conditional maximum:

$$(11.4) \quad \boldsymbol{\mu} = \arg \max_{\mathbf{u}} p(M', (\mathbf{k}_M, \mathbf{u})|\mathcal{D}).$$

A proposal centered at the posterior conditional maximum satisfies the first order condition:

$$(11.5) \quad \begin{aligned} \nabla \log A(M, \mathbf{k}_M \rightarrow M', \mathbf{k}_{M'}) \big|_{\boldsymbol{\mu}} &= \nabla [\log \mathcal{L}(\mathcal{D}; \mathbf{k}_M, \mathbf{u}) + \log p(\mathbf{k}_M, \mathbf{u}) \\ &\quad - \log q(\mathbf{u}; \boldsymbol{\mu}, \boldsymbol{\Sigma})] \big|_{\boldsymbol{\mu}} \\ &= \mathbf{0}. \end{aligned}$$

Further, setting the second-derivative of the acceptance ratio at the conditional maximum  $\mathbf{0}$ , we obtain the second order condition as:

$$\begin{aligned} \nabla^2 \log A((M, \mathbf{k}_M) \rightarrow (M', \mathbf{k}_{M'})) &= \nabla^2[\log \mathcal{L}(\mathbf{D} | \mathbf{k}_M, \mathbf{u}) + \log p(\mathbf{k}_M, \mathbf{u}) \\ &\quad - \log q(\mathbf{u}; \boldsymbol{\mu}, \boldsymbol{\Sigma})] \\ &= \mathbf{0}. \end{aligned} \tag{11.6}$$

Taking  $\mathcal{H}$  to be the Hessian of the conditional posterior density at  $\boldsymbol{\mu}$ , (11.6) yields

$$(11.7) \quad \mathcal{H}|_{\boldsymbol{\mu}} + \boldsymbol{\Sigma}^{-1} = \mathbf{0} \implies \boldsymbol{\Sigma} = -\mathcal{H}^{-1}|_{\boldsymbol{\mu}}.$$

**11.2. Network-aware parameter proposals.** The above proposal construction for between-model moves in which the parameter proposals adapt to conditional posterior densities typically lead to improved reversible jump simulations [2, 3, 4, 5]. Effectively, the above proposal construction is attempting to increase the chance of proposed moves between models to get accepted. In addition, with the first and second order conditions, the idea is to make acceptance ratio uniformly high for all transitions. However, the direct application of the centered second-order conditions for between-model moves in the context of reaction network inference has a major drawback. As discussed in the paper, many reaction networks can have the same effective network. In such a case, if the proposed move is between two networks with the same effective network (i.e., the two networks belong to the same cluster), the parameter proposal adapts to the prior distribution of the newly added reaction. We propose a network-aware approach in which, because we have determined the effective networks, we design parameter proposals that adapt to the difference between the effective networks of the two networks. When the proposed move is between two networks belonging to different clusters, we construct a proposal that approximates the conditional posterior distribution of the rate constants of all reactions *not included* in the two effective networks. Formally, suppose that the sampler proposes a move from a lower-dimensional model  $M$  to a higher-dimensional model  $M'$ . Let the effective networks of the two models  $M$  and  $M'$  be  $M_e$  and  $M'_e$ , respectively. Following our choice of the proposal  $q(M'|M)$ ,  $\dim(M') = \dim(M) + 1$ . Suppose the proposed move is such that  $M'_e \neq M_e$ , i.e., the effective networks of the current and the proposed networks are different. In our network-aware sampler, because we know the effective networks  $M'_e$  and  $M_e$  of the two models  $M'$  and  $M$ , respectively, we construct the following proposal:

$$(11.8) \quad \mathbf{f} := (\mathbf{k}_{M'_e}^{1:i}, \mathbf{k}_{M'_e}^{1:a}, \mathbf{w}_{M \setminus M_e}^{1:j}) = (\mathbf{k}_{M_e}^{1:i}, \mathbf{u}_{M_e}^{1:a}, \mathbf{k}_{M \setminus M_e}^{1:j}),$$

where  $\mathbf{u}_M^{1:a} \sim \mathcal{N}(\boldsymbol{\mu}_M, \boldsymbol{\Sigma}_M)$  and  $\mathbf{w}^{1:j} \sim p(\mathbf{k}_{M \setminus M_e}^{1:j} | M)$ . The proposal mean  $\boldsymbol{\mu}_M$ :

$$(11.9) \quad \boldsymbol{\mu}_M = \arg \max_{\mathbf{u}^{1:a}} p(\mathbf{u}^{1:a} | \mathbf{k}_{M_e}^{1:i}, M'_e, \mathbf{D})$$

is obtained by solving an  $a$ -dimensional optimization problem, where  $a$  is the difference between the number of reactions in the effective networks  $M'_e$  and  $M_e$ . The proposal covariance  $\boldsymbol{\Sigma}_M$ :

$$(11.10) \quad \boldsymbol{\Sigma}_M = -[\nabla \nabla \log p(\mathbf{u}^{1:a} | \mathbf{k}_{M_e}^{1:i}, M'_e, \mathbf{D})]^{-1}|_{\boldsymbol{\mu}_M},$$

is determined numerically using a finite-difference approximation at the proposal mean. Note  $p(\mathbf{k}_{M \setminus M_e}^{1:j} | M)$  is the prior probability density of reactions not in the effective network of  $M$ . The acceptance probability of the proposed move is given by

$$(11.11) \quad \alpha((M, \mathbf{k}_M), (M', \mathbf{k}'_{M'})) = \min \{1, A\},$$

where

$$(11.12) \quad A = \frac{p(M'_e, \mathbf{k}_{M'_e} | \mathcal{D}) q(M | M')}{p(M_e, \mathbf{k}_{M_e} | \mathcal{D}) q(M' | M) \mathcal{N}(\mathbf{u}_M^{1:a}; \boldsymbol{\mu}_M, \boldsymbol{\Sigma}_M)}.$$

The reverse move has an acceptance probability  $\min\{1, A^{-1}\}$ . The idea behind the construction of our network aware proposals is that by solving for the conditional maximum of the joint posterior density of the reactions  $M'_e \setminus M_e$  and determining the Hessian approximation at that point, we are building a Gaussian approximation of the conditional probability density  $p(\mathbf{k}'_e | \mathbf{k}_e, M'_e)$ . In contrast, the standard network-unaware approach would not; in particular the second-order condition of Brooks et al. [2] produces a proposal that is the product of prior densities for  $\dim(M'_e) - \dim(M_e) - 1$  rate constants and the conditional posterior distribution of the final  $a^{th}$  rate constant.

Method	Proposal
Network unaware	$q_{nu}(\mathbf{k}'_e \setminus \mathbf{k}_e) \approx \prod_{i=1}^{a-1} p(k^i) p(\mathbf{k}'_e \setminus \mathbf{k}^{1:a-1}   \mathbf{k}^{1:a-1}, M'_e, \mathcal{D})$
Network aware	$q_{na}(\mathbf{k}'_e \setminus \mathbf{k}_e) \approx p(\mathbf{k}'_e   \mathbf{k}_e, M'_e, \mathcal{D})$

TABLE 1. Cluster switching parameter proposals

Mathematically, the two proposals are shown in Table 1. The steps of our network-aware reversible jump MCMC algorithm are given in Algorithm 3. If we think of the cluster  $\{M_e, \mathbf{k}_e\}$  as the state space, the between-model moves that propose moves within the same cluster have an acceptance probability 1 with both the network-aware and the network-unaware approaches. However, when the proposed move is between two distinct clusters, our network aware approach chooses a proposal that approximates the joint conditional posterior density and hence leads to improved alignment between the densities  $p(\mathbf{k}_e | \mathcal{D}) q(\mathbf{u} | \mathbf{k}_e)$  and  $p(\mathbf{k}'_e | \mathcal{D})$  of the two spaces.

**11.3. Sensitivity-based network-aware proposals.** Between-model moves with deterministic reverse moves are a natural choice for nested models. However, in many cases, MCMC mixing may be improved by adopting non-deterministic reverse move types. In the context of reaction network inference, it is sometimes observed that a *maximum-a-posteriori* rate constant value for a reaction common to two networks differs substantially in the two networks. For example, consider the two networks in Figure 10. The most likely values for the rate constant of reaction  $*$  could differ significantly for the two networks. In such a case, keeping the rate constant of  $*$  fixed when proposing moves between the two networks leads to very poor acceptance rates. We propose a method to improve sampling efficiency of the network inference problem by identifying critical reactions common to the current and the proposed network and using a proposal distribution  $q$  for their rate constants in moves between the two networks. In other words, the reverse move from a high-dimensional effective

**Algorithm 3** Network-aware reversible jump MCMC

---

1: **Given:** A set of models  $M \in \mathcal{M}$  with corresponding parameter vectors  $\mathbf{k}_M$ , posterior densities  $p(M, \mathbf{k}_M | \mathcal{D})$ .  
2:  $\beta \in (0, 1)$ : probability of within-model move  
3: Initialize starting point  $(M^0, \mathbf{k}_{M^0})$   
4: **for**  $n = 0$  to  $N_{iter}$  **do**  
5:     Sample  $b \sim \mathcal{U}_{[0,1]}$   
6:     **if**  $b \leq \beta$  **then**  
7:         Metropolis-Hastings within-model move  
8:     **else**  
9:         Sample  $M' \sim q(M' | M^n = M)$ ;  $M'_e = \text{eff}(M')$  and  $M_e = \text{eff}(M)$   
10:         **if**  $|M'_e| > |M_e|$  **then**  

$$\boldsymbol{\mu}_M = \arg \max_{\mathbf{u}^{1:a}} p(\mathbf{u}^{1:a} | \mathbf{k}_{M_e}^{1:i}, M'_e, \mathcal{D}), \Sigma_M = -[\nabla^2 \log p(\mathbf{u}^{1:a} | \mathbf{k}_{M_e}^{1:i}, M'_e, \mathcal{D})]^{-1} \Big|_{\boldsymbol{\mu}_M}$$
11:         Sample  $\mathbf{u}_M^{1:a} \sim \mathcal{N}(\boldsymbol{\mu}_M, \Sigma_M)$   
12:         Set  $(\mathbf{k}_{M'_e}^{1:i}, \mathbf{k}_{M'_e}^{1:a}, \mathbf{w}_{M' \setminus M'_e}^{1:j}) = (\mathbf{k}_{M_e}^{1:i}, \mathbf{u}_M^{1:a}, \mathbf{k}_{M' \setminus M'_e}^{1:j})$   
13:          $\alpha((M, \mathbf{k}_M), (M', \mathbf{k}'_{M'})) = \min \left\{ 1, \frac{p(M'_e, \mathbf{k}_{M'_e} | \mathcal{D}) q(M | M')}{p(M_e, \mathbf{k}_{M_e} | \mathcal{D}) q(M' | M) \mathcal{N}(\mathbf{u}_M^{1:a}; \boldsymbol{\mu}_M, \Sigma_M)} \right\}$   
14:         **else if**  $|M'_e| < |M_e|$  **then**  

$$\boldsymbol{\mu}_{M'} = \arg \max_{\mathbf{u}^{1:a}} p(\mathbf{u}^{1:a} | \mathbf{k}_{M_e}^{1:i}, M_e, \mathcal{D}), \Sigma_{M'} = -[\nabla^2 \log p(\mathbf{u}^{1:a} | \mathbf{k}_{M_e}^{1:i}, M_e, \mathcal{D})]^{-1} \Big|_{\boldsymbol{\mu}_M}$$
15:         Sample  $\mathbf{w}_{M' \setminus M'_e}^{1:j} \sim p(\mathbf{k}_{M' \setminus M'_e}^{1:j} | M')$   
16:         Set  $(\mathbf{k}_{M'_e}^{1:i}, \mathbf{u}_{M' \setminus M'_e}^{1:a}, \mathbf{k}_{M' \setminus M'_e}^{1:j}) = (\mathbf{k}_{M_e}^{1:i}, \mathbf{k}_{M' \setminus M'_e}^{1:a}, \mathbf{w}_{M' \setminus M'_e}^{1:j})$   
17:          $\alpha((M, \mathbf{k}_M), (M', \mathbf{k}'_{M'})) = \min \left\{ 1, \frac{p(M'_e, \mathbf{k}_{M'_e} | \mathcal{D}) q(M | M') \mathcal{N}(\mathbf{u}_{M'}^{1:a}; \boldsymbol{\mu}_{M'}, \Sigma_{M'})}{p(M_e, \mathbf{k}_{M_e} | \mathcal{D}) q(M' | M)} \right\}$   
18:         **else**  
19:         Sample  $\mathbf{w}_{M' \setminus M'_e}^{1:j} \sim p(\mathbf{k}_{M' \setminus M'_e}^{1:j} | M')$   
20:         Set  $(\mathbf{k}_{M'_e}^{1:i}, \mathbf{u}_{M' \setminus M'_e}^{1:a}, \mathbf{k}_{M' \setminus M'_e}^{1:j}) = (\mathbf{k}_{M_e}^{1:i}, \mathbf{k}_{M' \setminus M'_e}^{1:a}, \mathbf{w}_{M' \setminus M'_e}^{1:j})$   
21:          $\alpha((M, \mathbf{k}_M), (M', \mathbf{k}'_{M'})) = 1$   
22:         Sample  $p \sim \mathcal{U}_{[0,1]}$   
23:         **if**  $p < \alpha((M, \mathbf{k}_M), (M', \mathbf{k}'_{M'}))$  **then**  
24:              $(M^{n+1}, \mathbf{k}_{M^{n+1}}^{n+1}) = (M', \mathbf{k}_{M'}^{n+1})$   
25:         **else**  
26:              $(M^{n+1}, \mathbf{k}_{M^{n+1}}^{n+1}) = (M^n, \mathbf{k}_{M^n}^n)$

---

network to a low-dimensional effective network is no longer deterministic. The move between the networks takes the following form:

$$(11.13) \quad (\mathbf{k}_{M'_e}, \mathbf{u}'_e) = \mathbf{f}(\mathbf{k}_{M_e}, \mathbf{u}_e).$$

The question we answer next is how one could identify “key” reactions whose inclusion in the proposal would improve MCMC mixing at a limited computational overhead. Given a set of observables and the current and proposed network, a useful strategy is to identify the reactions to which the posterior density is most sensitive. To determine the sensitivity of the posterior density to individual reactions given a network, we employ local sensitivity analysis. Say, we have network  $M$  with reactions

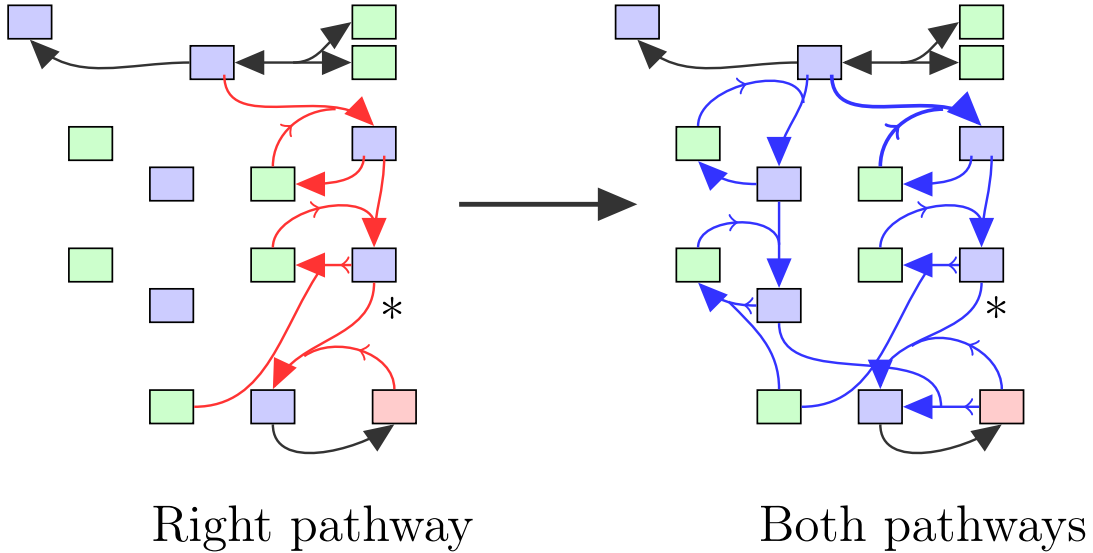


FIGURE 10. Two networks with different pathways

$R_1, R_2, \dots, R_M$ . We determine the expected local sensitivity index  $\mathbb{E} \left[ \left| \frac{\partial \log p(k_i | \mathcal{D}, \mathbf{k}_{-i})}{\partial k_i} \right| \right]$  of reaction  $i$  with  $\mathbf{k}_{-i}^*$  given nominal values and the expectation taken with respect to the prior distribution  $p(k_i | M)$ . In practice, since the expectation is usually not analytically tractable, we settle for a noisy estimate of the expectation by evaluating the local sensitivity at a few realizations from the prior distribution and taking their average. Having determined the sensitivity of the log-posterior of the current and the proposed reaction network, we select a random number of high sensitivity reactions common to the two networks and include proposals for their rate constants in the forward and the reverse moves. The choice of the number of reactions to be included in the proposals is based on a Poisson distribution whose mean is kept at a small value. Choosing to include only a few common rate constant into the proposal is again based on the understanding that constructing effective proposals in high dimensions is generally hard. Thus, as the jump function for moves between models  $M$  and  $M'$  we have

$$(11.14) \quad f := (k_{M'}^{1:i}, k_{M'}^{1:a}, k_{M'}^{1:c}, u'^{1:c}) = (k_M^{1:i}, u_M^{1:a}, u^{1:c}, k_M^{1:c}).$$

Here,  $\{1 : i\}$  are indices of reactions whose parameter values are kept fixed during moves between models  $M$  and  $M'$ ,  $\{1 : a\}$  are indices of reactions that are in model  $M'$  but not in  $M$ , and  $\{1 : c\}$  are reactions that are present in both models but whose rate constant values are determined according to respective proposal distributions. Next, the parameter proposals  $q(\mathbf{u}_M^{1:a}, \mathbf{u}_M^{1:c} | \mathbf{k}_M^{1:i})$  and  $q(\mathbf{u}'^{1:c} | \mathbf{k}_{M'}^{1:i})$  are again chosen as Gaussian approximations of the conditional posteriors  $p(\mathbf{k}_{M'}^{1:a}, \mathbf{k}_{M'}^{1:c} | \mathbf{k}_{M'}^{1:i}, \mathcal{D})$  and  $p(\mathbf{k}_M^{1:c} | \mathbf{k}_M^{1:i}, \mathcal{D})$ , respectively. Note, this construction of parameter proposals improves alignment between densities  $p(\mathbf{k}_{M'}^{1:i}, \mathbf{k}_{M'}^{1:a}, \mathbf{k}_{M'}^{1:c} | M', \mathcal{D})q(\mathbf{u}'^{1:c})$  and  $p(\mathbf{k}_M^{1:i}, \mathbf{k}_M^{1:c} | M, \mathcal{D})q(\mathbf{u}_M^{1:a}, \mathbf{u}_M^{1:c})$  and produces efficient reversible jump proposals. The above construction of reversible jump proposals satisfies the second-order conditions of Brooks et al [2]. The foregoing discussion has focused on a network-unaware approach, where the effective networks are not known apriori. As we discussed in Section 11.2 on

network-aware proposals, for the network inference problem, improved proposals that approximate the joint posterior conditionals of the rate constants of the difference in reactions between the current and proposed effective networks can be constructed by determining the effective networks of proposed networks. We combine the network-aware scheme of the previous section with the sensitivity-based determination of move types to yield the the *sensitivity-based network-aware proposals*. The sequence of steps for our sensitivity-based network-aware reversible jump MCMC algorithm are given in Algorithm 4.

---

**Algorithm 4** Sensitivity-based network-aware reversible jump MCMC

---

- 1: **Given:** A set of models  $M \in \mathcal{M}$  with corresponding parameter vectors  $\mathbf{k}_M$ , posterior densities  $p(M, \mathbf{k}_M | \mathcal{D})$ .
- 2:  $\beta \in (0, 1)$ : probability of within-model move
- 3: Initialize starting point  $(M^0, \mathbf{k}_{M^0})$
- 4: **for**  $n = 0$  to  $N_{iter}$  **do**
- 5:     Sample  $b \sim \mathcal{U}_{[0,1]}$
- 6:     **if**  $b \leq \beta$  **then**
- 7:         Metropolis-Hastings within-model move
- 8:     **else**
- 9:         Sample  $M' \sim q(M' | M^n = M)$ ;  $M'_e = \text{eff}(M')$  and  $M_e = \text{eff}(M)$
- 10:          $r_1 \sim \text{Poisson}(1.5)$  and  $r_2 \sim \text{Poisson}(1.5)$
- 11:          $\{1 : c\}$ =reactions with top  $r_1$  and  $r_2$  sensitivities of  $M_e$  and  $M'_e$ , respectively, and common to  $M_e$  and  $M'_e$ .
- 12:         **if**  $|M'_e| > |M_e|$  **then**
- 13:              $\boldsymbol{\mu}_{M_e} = \arg \max_{\mathbf{u}^{1:a}, \mathbf{u}^{1:c}} p(\mathbf{u}^{1:a}, \mathbf{u}^{1:c} | \mathbf{k}_{M_e}^{1:i}, M'_e, \mathcal{D})$ ,  $\boldsymbol{\Sigma}_{M_e} = -[\nabla^2 \log p(\mathbf{u}^{1:a}, \mathbf{u}^{1:c} | \mathbf{k}_{M_e}^{1:i}, M'_e, \mathcal{D})]^{-1} |_{\boldsymbol{\mu}_M}$
- 14:              $\boldsymbol{\mu}_{M'_e} = \arg \max_{\mathbf{u}^{1:c}} p(\mathbf{u}^{1:c} | \mathbf{k}_{M_e}^{1:i}, M_e, \mathcal{D})$ ,  $\boldsymbol{\Sigma}_{M'_e} = -[\nabla^2 \log p(\mathbf{u}^{1:c} | \mathbf{k}_{M_e}^{1:i}, M_e, \mathcal{D})]^{-1} |_{\boldsymbol{\mu}_{M'}}$
- 15:             Sample  $\mathbf{u}^{1:a}, \mathbf{u}^{1:c} \sim \mathcal{N}(\boldsymbol{\mu}_{M_e}, \boldsymbol{\Sigma}_{M_e})$
- 16:             Set  $(\mathbf{k}_{M'_e}^{1:i}, \mathbf{k}_{M'_e}^{1:a}, \mathbf{k}_{M'_e}^{1:c}, \mathbf{u}'^{1:c}) = (\mathbf{k}_{M_e}^{1:i}, \mathbf{u}^{1:a}, \mathbf{u}^{1:c}, \mathbf{k}_{M_e}^{1:c})$
- 17:         **else if**  $|M'_e| < |M_e|$  **then**
- 18:              $\boldsymbol{\mu}_{M_e} = \arg \max_{\mathbf{u}^{1:c}} p(\mathbf{u}^{1:c} | \mathbf{k}_{M_e}^{1:i}, M'_e, \mathcal{D})$ ,  $\boldsymbol{\Sigma}_{M_e} = -[\nabla^2 \log p(\mathbf{u}^{1:c} | \mathbf{k}_{M_e}^{1:i}, M'_e, \mathcal{D})]^{-1} |_{\boldsymbol{\mu}_M}$
- 19:              $\boldsymbol{\mu}_{M'_e} = \arg \max_{\mathbf{u}^{1:a}, \mathbf{u}^{1:c}} p(\mathbf{u}^{1:a}, \mathbf{u}^{1:c} | \mathbf{k}_{M_e}^{1:i}, M_e, \mathcal{D})$ ,  $\boldsymbol{\Sigma}_{M'_e} = -[\nabla^2 \log p(\mathbf{u}^{1:a}, \mathbf{u}^{1:c} | \mathbf{k}_{M_e}^{1:i}, M_e, \mathcal{D})]^{-1} |_{\boldsymbol{\mu}_{M'}}$
- 20:             Sample  $\mathbf{u}^{1:c} \sim \mathcal{N}(\boldsymbol{\mu}_{M_e}, \boldsymbol{\Sigma}_{M_e})$
- 21:             Set  $(\mathbf{k}_{M'_e}^{1:i}, \mathbf{u}'^{1:a}, \mathbf{u}'^{1:c}, \mathbf{k}_{M'_e}^{1:c}) = (\mathbf{k}_{M_e}^{1:i}, \mathbf{k}_{M_e}^{1:a}, \mathbf{k}_{M_e}^{1:c}, \mathbf{u}^{1:c})$
- 22:         **else**  $\boldsymbol{\mu}_{M_e} = \emptyset$ ,  $\boldsymbol{\mu}_{M'_e} = \emptyset$ ,  $\boldsymbol{\Sigma}_{M_e} = \emptyset$ ,  $\boldsymbol{\Sigma}_{M'_e} = \emptyset$
- 23:         Sample  $\mathbf{k}_{M' \setminus M'_e}^{1:j} \sim p(\mathbf{k}_{M' \setminus M'_e}^{1:j} | M')$
- 24:         Sample  $p \sim \mathcal{U}_{[0,1]}$
- 25:         **if**  $p < \min \left\{ 1, \frac{p(M'_e, \mathbf{k}_{M'_e} | \mathcal{D})q(M^n | M')\mathcal{N}(\mathbf{u}' | \boldsymbol{\mu}_{M'_e}, \boldsymbol{\Sigma}_{M'_e})}{p(M_e, \mathbf{k}_{M_e} | \mathcal{D})q(M' | M^n)\mathcal{N}(\mathbf{u} | \boldsymbol{\mu}_{M_e}, \boldsymbol{\Sigma}_{M_e})} \right\}$  **then**
- 26:              $(M^{n+1}, \mathbf{k}_{M^{n+1}}^{n+1}) = (M', \mathbf{k}_{M'})$
- 27:         **else**
- 28:              $(M^{n+1}, \mathbf{k}_{M^{n+1}}^{n+1}) = (M^n, \mathbf{k}_{M^n}^n)$

---

**11.4. Derandomization of conditional expectations.** The above Algorithms 3 and 4 lead to gains in sampling efficiency compared to a reversible jump MCMC algorithm that does not use information on network structure in designing between-model moves and parameter proposals. Identifying clusters of models can be further

used for additional variance reduction. With the knowledge that all models belonging to the same cluster have identical model evidence, we can compute some expectations analytically and thereby obtain posterior averages of features with lower variances.

11.4.1. *General formulation.* Let us assume we performing model inference with  $F$  as one the quantities of interest. Generally, we may be interested in quantities such as the posterior model probabilities, reaction inclusion probabilities of reactions, or pathway probabilities. The Monte Carlo estimate of  $F$  from posterior samples can be written as:

$$\begin{aligned}\hat{F} &= p(F = 1|\mathcal{D}) \\ &= \int p(F = 1|C)p(C|\mathcal{D})dC \\ &= \int p(F = 1|M)p(M|C)p(C|\mathcal{D})dMdC \\ &= \int \mathbb{E}_{p(M|C)} [p(F = 1|M)] p(C|\mathcal{D})dC \\ &= \frac{1}{N_s} \sum_{i=1}^{N_s} \mathbb{E}_{p(M|C^i)} [p(F = 1|M)],\end{aligned}$$

where  $C$  refers to model clusters,  $N_s$  is the number of posterior samples and  $\mathcal{D}$  the available data. In the above equation,  $\mathbb{E}_{p(M|C^i)}[p(F = 1|M)]$  is the expected value of  $p(F = 1|M)$  conditioned on the generated sample  $C^i$ . Knowing the cluster to which each sample belongs and the dependence of the feature on the models included in the cluster, the above expectation can be computed analytically and allows variance reduction. In contrast, in the network-unaware approach, the expectation is computed through Monte Carlo sampling.

11.4.2. *Example: model probability estimates.* Consider that the feature of interest is the probability of model  $m$ . Thus, applying the above formula to the estimation of model probability, we get

$$\begin{aligned}\hat{M}_m &= p(M_m = 1|\mathcal{D}) \\ &= \int p(M_m = 1|C)p(C|\mathcal{D})dC \\ &= \int p(M_m = 1|M)p(M|C)p(C|\mathcal{D})dMdC \\ &= \int \mathbb{E}_{p(M|C)} [p(M_m = 1|M)] p(C|\mathcal{D})dC \\ &= \frac{1}{N_s} \sum_{i=1}^{N_s} \mathbb{E}_{p(M|C^i)} [p(M_m = 1|M)] \\ (11.15) \quad &= \frac{1}{N_s} \sum_{i=1}^{N_s} p(M_m|C_K) \mathbb{1}_{C_K}(C^i),\end{aligned}$$

where  $K : \mathbb{1}_{M_m \in C_K}(M_m) = 1$  and  $\mathbb{1}$  is the indicator function. In our network aware schemes,  $p(M_m|C_K)$  can be computed analytically. For example, for a cluster  $C_K$

with  $N_K$  models, taking the prior distribution over models to be uniform, the model probability estimate is

$$(11.16) \quad \hat{M}_m = \frac{1}{N_s} \sum_{i=1}^{N_s} \frac{1}{N_K} \mathbb{1}_{C_K}(C^i)$$

In contrast, with a standard reversible-jump algorithm, the model probability estimate is

$$(11.17) \quad \hat{M}_m = \frac{1}{N_s} \sum_{i=1}^{N_s} \mathbb{1}_{M_m}(M^i) \mathbb{1}_{C_K}(C^i)$$

## 12. RESULTS

In our paper, we present two example problems and demonstrate the efficiency of our network-aware sampling approaches compared to the network-unaware second-order approach of Brooks et al [2]. The observables in our examples are species concentrations and the concentration evolution is modeled using the law of mass action/Michaelis-Menten functionals. The resulting nonlinear system of ordinary differential equations are solved using the multistep BDF integrator available in the SUNDIALS suite [8].

**12.1. Example 1: five-dimensional nonlinear network inference.** As our first example, we consider a five-dimensional nonlinear network inference problem where the species interactions are governed by the law of mass action (Figure 11). The law of mass action gives the rate of a chemical reaction (say  $X + Y \rightarrow Z$ ) as the product of a reaction-specific rate constant  $k$  with reactant concentrations  $[X]$  and  $[Y]$ :

$$(12.1) \quad \text{Rate} = -k[X][Y].$$

Under some assumptions, the law of mass action produces Michaelis-Menten reaction rate expression

$$(12.2) \quad \text{Rate} = \frac{k[S]}{k_M + [S]},$$

or when enzyme concentration is taken into account [10]:

$$(12.3) \quad \text{Rate} = k[E]_0 \frac{[S]}{k_M + [S]},$$

where  $k$  denotes the rate constant,  $[E]_0$  is the enzyme concentration,  $[S]$  the substrate concentration, and  $k_M$  the Michaelis constant.

In the present example, we consider a subset of reactions (15 species and 12 reactions) proposed for a protein-signalling network of the activation of extracellular signal-regulated kinase (ERK) by epidermal growth factor (EGF) (Figure 11) [11]. The ODE forward model governing the evolution of species concentrations is described in detail in Section 13. We keep reactions 1, 2, 8, 9, 10, 11, and 12 fixed (denoted by thick lines in the reaction graph 11 and shaded pink in Table 2) and

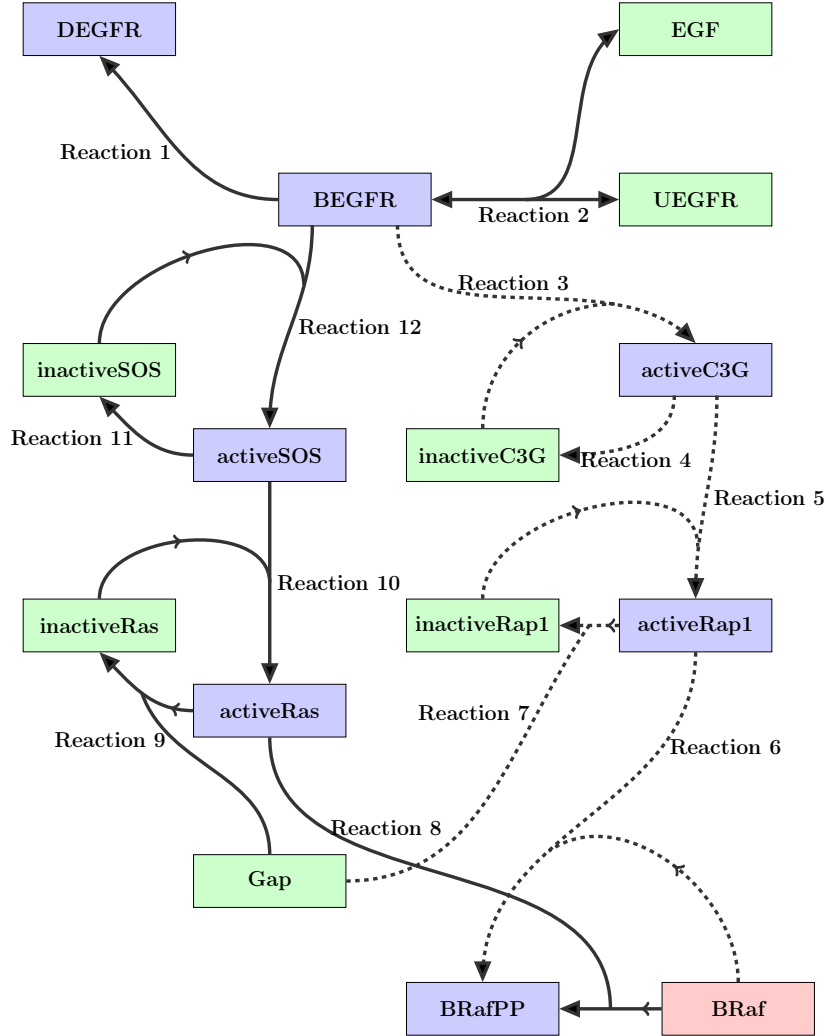


FIGURE 11. A reaction network with 5 (reactions 3, 4, 5, 6, and 7) uncertain reactions. BRaf is the observable.

thus they are included in all the inferred models. The rate constants of all fixed reactions and Michaelis constants of all reactions are set to their base values (Table 2). Reactions 3, 4, 5, 6, and 7 are taken to be uncertain and the concentration of BRaf is taken to be the observable. With the above five uncertain reactions, the number of potential models is 32. And with only BRaf as the observable, the number of clusters is 5. The resulting problem is a nonlinear network inference problem for which the marginal likelihood is not analytically computable.

We generated 20 i.i.d. data points with noise model  $\mathcal{N}(0, 4)$  and rate constants and Michaelis constants set to their base values (Table 2). We impose independent Gaussian priors on the rate constants of the uncertain reactions with means and variances as shown in Table 2. The above prior amounts to roughly three orders of magnitude prior uncertainty in the rate constants. All models are assigned a

	Reaction	$\log_{10} k^*{}^a$	$k_M^b$	Prior uncertainty
1	$\text{BEGFR} \rightarrow \text{DEGFR}$	0.0	-	—
2a	$\text{EGF} + \text{UEGFR} \rightarrow \text{BEGFR}$	1.5	-	—
2b	$\text{BEGFR} \rightarrow \text{EGF} + \text{UEGFR}$	0.0	-	—
3	$\text{inactiveC3G} + \text{BEGFR} \rightarrow \text{activeC3G} + \text{BEGFR}$	0.5	3386.3875	$\log_{10} k = \mathcal{N}(1.1, 0.2)$
4	$\text{activeC3G} \rightarrow \text{inactiveC3G}$	2.0	-	$\log_{10} k = \mathcal{N}(1.4, 0.2)$
5	$\text{inactiveRap1} + \text{activeC3G} \rightarrow \text{activeRap1} + \text{activeC3G}$	2.0	3566	$\log_{10} k = \mathcal{N}(2.6, 0.2)$
6	$\text{BRaf} + \text{activeRap1} \rightarrow \text{BRafPP} + \text{activeRap1}$	0.4	17991.179	$\log_{10} k = \mathcal{N}(1.0, 0.2)$
7	$\text{activeRap1} + \text{Gap} \rightarrow \text{inactiveRap1} + \text{Gap}$	1.0	6808.32	$\log_{10} k = \mathcal{N}(0.4, 0.2)$
8	$\text{BRaf} + \text{activeRas} \rightarrow \text{BRafPP} + \text{activeRas}$	0.5	7631.63	—
9	$\text{activeRas} + \text{Gap} \rightarrow \text{inactiveRas} + \text{Gap}$	0.0	12457.816	—
10	$\text{inactiveRas} + \text{activeSOS} \rightarrow \text{activeRas} + \text{activeSOS}$	0.5	13.73	—
11	$\text{activeSOS} \rightarrow \text{inactiveSOS}$	4.0	9834.13	—
12	$\text{inactiveSOS} + \text{BEGFR} \rightarrow \text{activeSOS} + \text{BEGFR}$	2.5	8176.56	—

<sup>a</sup> logarithm (base rate constant value)

<sup>b</sup> Base value of Michaelis constant (Obtained from Xu et al. [11])

TABLE 2. Proposed reactions for Example 1

uniform prior probability. The noise variance for the likelihood function, as in the data generating process, is taken as  $\sigma^2 = 4$ .

We compare the sampling efficiency of our network-aware algorithm (Section 11.2) to the network-unaware 2<sup>nd</sup> order proposal of Brooks et al [2]. We simulated 5 replications of 400000 samples using both the approaches. 30000 samples each were discarded as burn-in. All simulations produce similar posterior inferences, thereby indicating convergence. Figure 12 shows samples generated from the posterior distribution using the two approaches color coded according to the pathway they belong. Blue points are posterior samples from all models that belong to the left pathway, i.e., models that do not contain any of reactions 3, 5, and 6. Orange points are posterior samples from models that operate with both—left and right branch—pathways, i.e., models that necessarily include reactions 3, 5, 6, 8, 10 and 12. The higher frequency of moves between the left pathway models and both pathways models with the network-aware approach is a sign of faster posterior exploration and consequently better MCMC mixing. Table 3 shows the acceptance rates of between models moves and between-cluster moves for the two approaches. High model-switching and cluster-switching acceptance rates with the same posterior inference is an indication of superior mixing of the network-aware approach. Effective sample size (ESS) calculation for statistics that retain interpretation throughout the simulation is another diagnostic for MCMC mixing. Effective sample size gives the equivalent number of independent samples to the dependent MCMC samples obtained in terms of learning the particular statistic. We take the number of reactions in the models as the quantity whose ESS is compared. In Table 3, we present the ESS for the number-of-reactions-in-model statistic. The network-aware scheme has a ten-fold higher ESS compared to the network-unaware approach. A more useful comparison of the two schemes would be to compare the number of effective samples per unit time because it also incorporates the computational time. The ESS per minute diagnostic in the last column of Table 3 confirms favourability of the network-aware approach with the computational cost taken into account. The absolute value of ESS per minute depends on the relative and absolute tolerance settings of the ODE solver. In particular, we chose very tight tolerances, but higher ESS/min can be obtained with loose

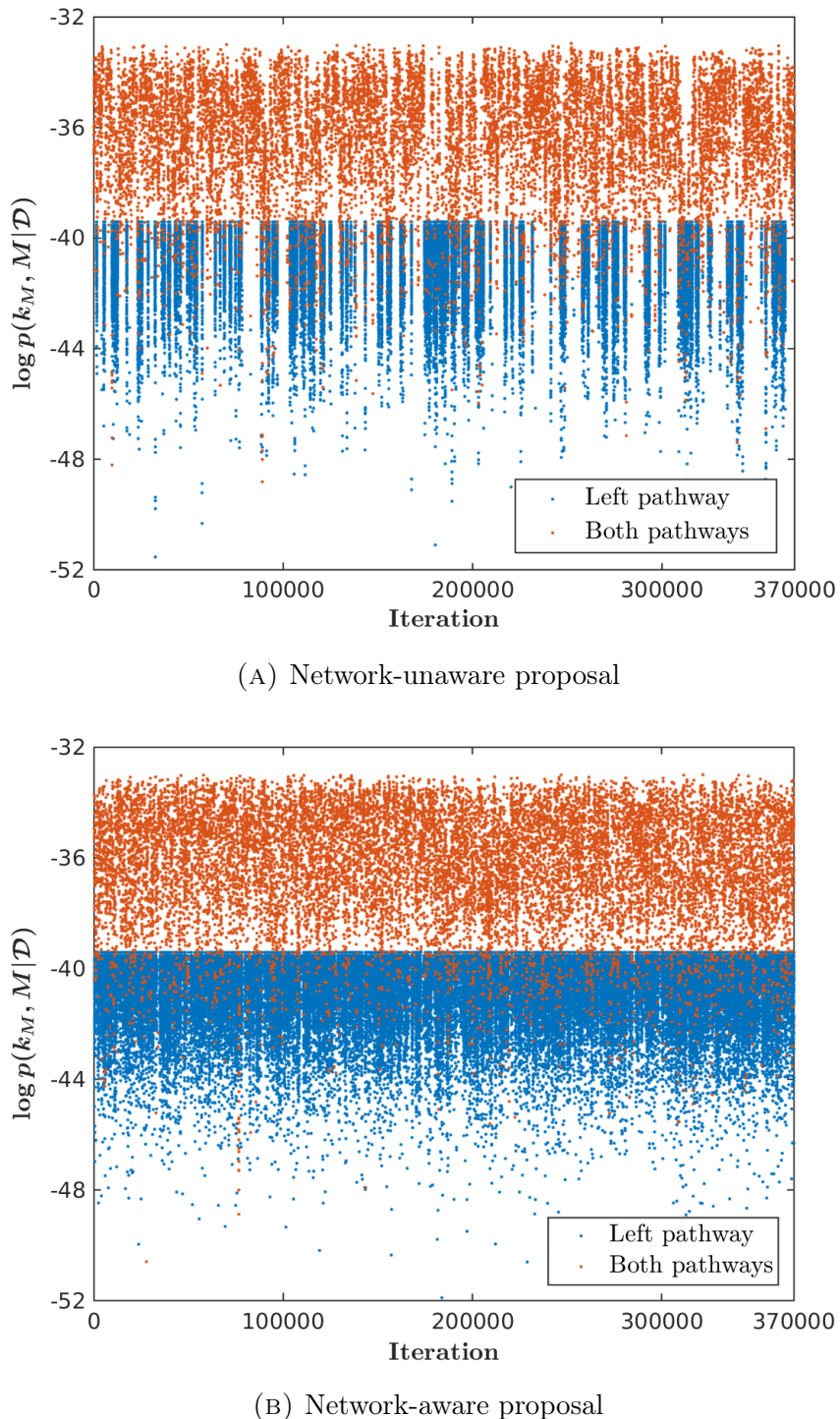


FIGURE 12. MCMC trace plots for Example 1: posterior samples from models with both pathways in orange and samples from models with only the left pathway in blue

tolerances. Nonetheless, the relative values of ESS/min demonstrate the advantage of using the network-aware sampling approach.

Method <sup>†</sup>	$p(M)^a$	$\bar{\alpha}_M^b$	$\bar{\alpha}_C^c$	ESS <sup>d</sup>	ESS/min <sup>e</sup>
Network unaware	0.7545	0.19	0.015	10	0.175
Network aware	0.7544	0.22	0.034	110	0.301

<sup>†</sup>: Performance is averaged over 5 simulation runs

<sup>a</sup>: Posterior probability of the data-generating model

<sup>b</sup>: Between-model move acceptance rate

<sup>c</sup>: Between-cluster move acceptance rate

<sup>d</sup>: Effective sample size for 10000 samples

<sup>e</sup>: The absolute values depend on the tolerances chosen for the ODE solver

TABLE 3. Summary statistics of MCMC simulations (Example 1).

**12.2. Example 2: ten-dimensional nonlinear network inference.** Our second example is a large scale nonlinear network inference problem with 10 uncertain reactions. Once again, we consider a protein-signalling network consisting of 15 species and 12 potential species interactions (Figure 13). The ODE forward model governing the evolution of species concentrations is described in detail in Section 13. We keep only reactions 1 and 2 fixed (denoted by thick lines in the reaction graph 13 and shaded pink in Table 4) and thus they are included in all the inferred models. The rate constants of all fixed reactions and Michaelis constants of all reactions are set to their base values (Table 4). Reactions 3–12 are uncertain and the concentration of BRaf is again the observable. With the above ten uncertain reactions, the number of potential models is 1024. And with only BRaf as the observable, the number of clusters is 24.

	Reaction	$\log_{10} k^*{}^a$	$k_M^b$	Prior uncertainty
1	BEGFR $\rightarrow$ DEGFR	0.0	-	—
2a	EGF + UEGFR $\rightarrow$ BEGFR	1.5	-	—
2b	BEGFR $\rightarrow$ EGF + UEGFR	0.0	-	—
3	inactiveC3G+BEGFR $\rightarrow$ activeC3G+BEGFR	0.5	3386.3875	$\log_{10} k = \mathcal{N}(1.2, 0.1)$
4	activeC3G $\rightarrow$ inactiveC3G	2.0	-	$\log_{10} k = \mathcal{N}(2.0, 0.1)$
5	inactiveRap1+activeC3G $\rightarrow$ activeRap1+activeC3G	2.0	3566	$\log_{10} k = \mathcal{N}(2.7, 0.1)$
6	BRaf+activeRap1 $\rightarrow$ BRafPP+activeRap1	0.4	17991.179	$\log_{10} k = \mathcal{N}(1.1, 0.1)$
7	activeRap1+Gap $\rightarrow$ inactiveRap1+Gap	1.0	6808.32	$\log_{10} k = \mathcal{N}(1.0, 0.01)$
8	BRaf+activeRas $\rightarrow$ BRafPP+activeRas	0.5	7631.63	$\log_{10} k = \mathcal{N}(0.5, 0.1)$
9	activeRas+Gap $\rightarrow$ inactiveRas+Gap	0.0	12457.816	$\log_{10} k = \mathcal{N}(0.0, 0.01)$
10	inactiveRas+activeSOS $\rightarrow$ activeRas+activeSOS	0.5	13.73	$\log_{10} k = \mathcal{N}(0.5, 0.1)$
11	activeSOS $\rightarrow$ inactiveSOS	4.0	9834.13	$\log_{10} k = \mathcal{N}(4.0, 0.01)$
12	inactiveSOS+BEGFR $\rightarrow$ activeSOS+BEGFR	2.5	8176.56	$\log_{10} k = \mathcal{N}(2.5, 0.1)$

<sup>a</sup> logarithm (base rate constant value)

<sup>b</sup> Base value of Michaelis constant (Obtained from Xu et al. [11])

TABLE 4. Proposed reactions for Example 2

We generated 30 i.i.d. data points with noise model  $\mathcal{N}(0, 0.04)$  and all rate constants and Michaelis constants set to their base values (Table 4). We impose independent Gaussian priors on the rate constants of the uncertain reactions with means and variances as shown in Table 4. The prior probability distribution over all plausible models is taken to be uniform. The noise variance for the likelihood function, as in the data generating process, is taken as  $\sigma^2 = 0.04$ .

Figure 14 shows samples generated (after a burn-in of 300000 samples) from the posterior distribution using our sensitivity-based network-aware algorithm (Section

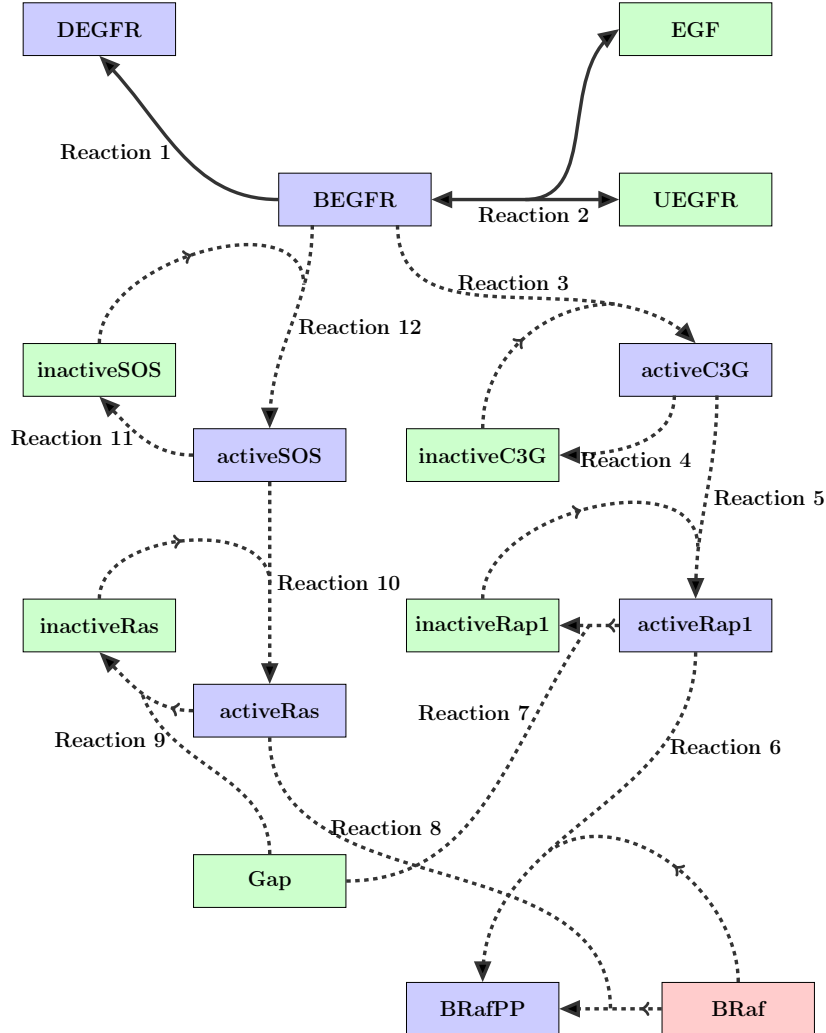
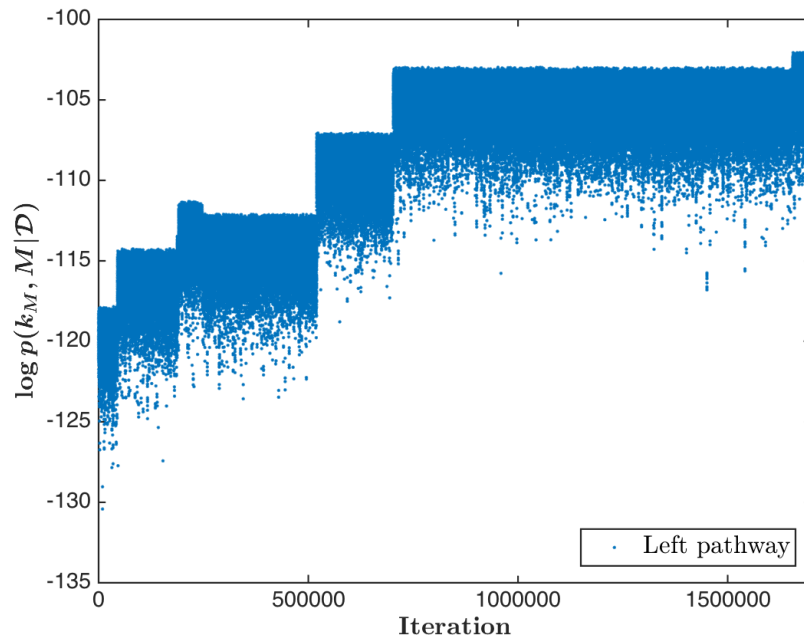
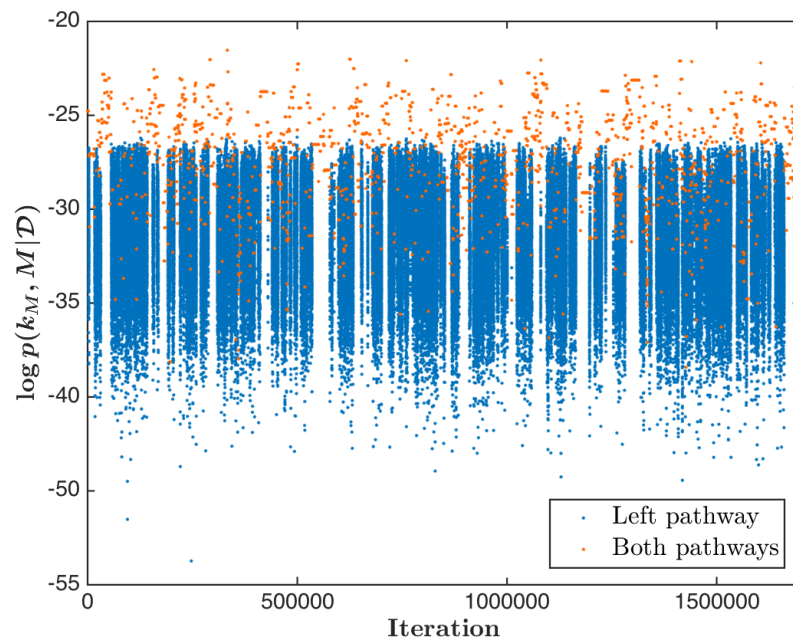


FIGURE 13. A reaction network with 10 (reactions 2–12) uncertain reactions. BRaf is the observable.

11.3) and the network-unaware 2<sup>nd</sup> order proposal of Brooks et al. [2], which are color coded according to the pathway they belong. Blue points are posterior samples from all models that belong to the left pathway, i.e., models that do not contain any of reactions 3, 5, and 6. Orange points are posterior samples from models that operate with both—left and right branch—pathways, i.e., models that necessarily include reactions 3, 5, 6, 8, 10 and 12. We see that even after 2 million samples are generated, the samplers remain confined to the models from the left pathway without ever switching to models with both pathways. In contrast, we observe that our sensitivity-based network-aware algorithm has a high frequency of moves between the left-pathway models and both-pathways models, indicating efficient posterior exploration.



(A) Network-unaware proposal



(B) Sensitivity-based network-aware proposal

FIGURE 14. MCMC trace plots for Example 2: posterior samples from models with both pathways in orange and samples from models with only the left pathway in blue

## 13. 12-DIMENSIONAL REACTION NETWORK

Here we present the details of the set of proposed reactions, the corresponding reaction and species production rate ODE expressions for the 12-reaction network used in Example 1 and Example 2.

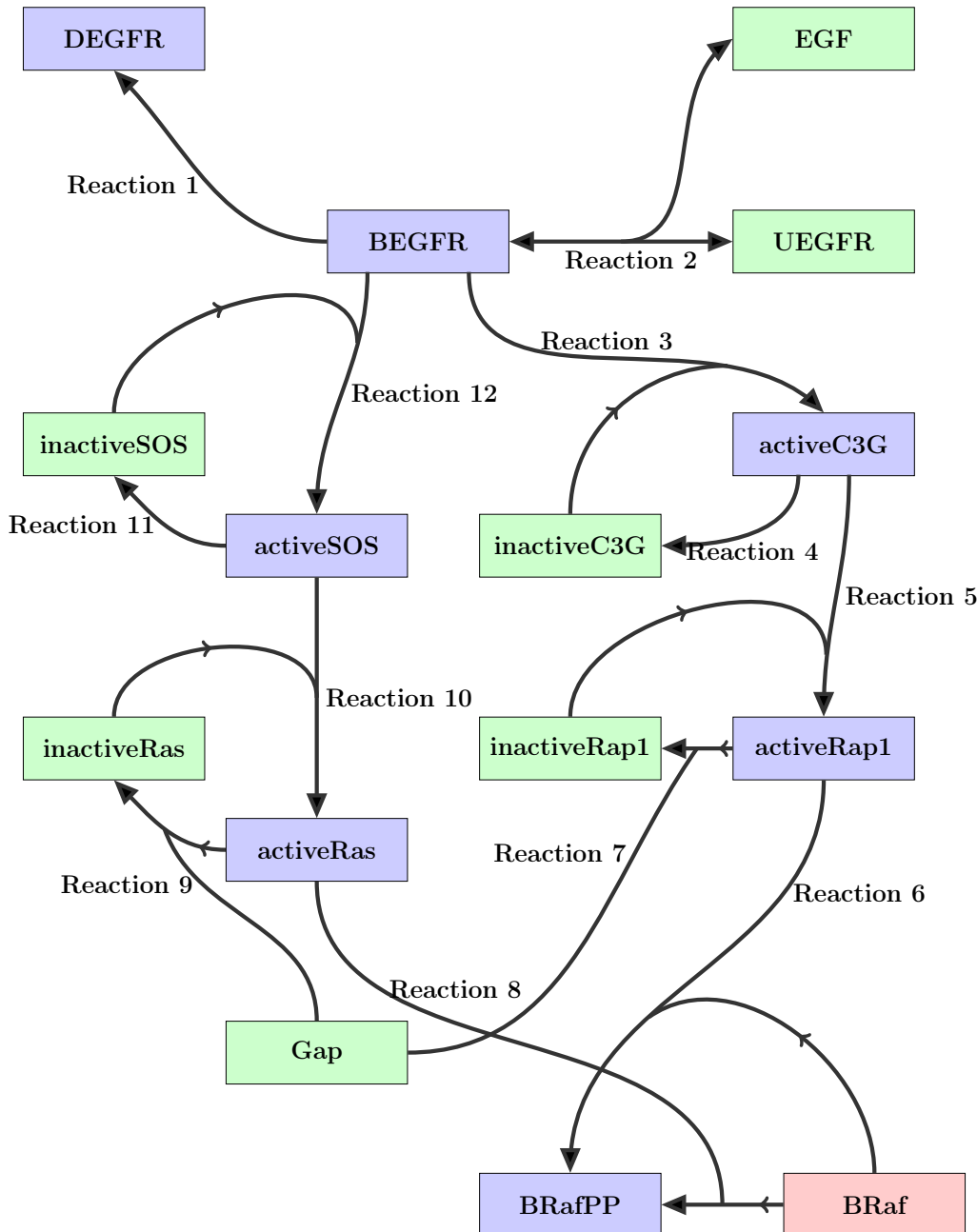


FIGURE 15. 12-reaction network of Example 1 and 2

### 13.1. Reactions.

1.  $boundEGFR \rightarrow degradedEGFR$
2.  $EGF + unboundEGFR \leftrightarrow boundEGFR$
3.  $inactiveC3G + boundEGFR \rightarrow activeC3G + boundEGFR$
4.  $activeC3G \rightarrow inactiveC3G$
5.  $inactiveRap1 + activeC3G \rightarrow activeRap1 + activeC3G$
6.  $BRaf + activeRap1 \rightarrow BRafPP + activeRap1$
7.  $activeRap1 + Gap \rightarrow inactiveRap1 + Gap$
8.  $BRaf + activeRas \rightarrow BRafPP + activeRas$
9.  $activeRas + Gap \rightarrow inactiveRas + Gap$
10.  $inactiveRas + activeSOS \rightarrow activeRas + activeSOS$
11.  $activeSOS \rightarrow inactiveSOS$
12.  $inactiveSOS + boundEGFR \rightarrow activeSOS + boundEGFR$

### 13.2. Reaction rates.

1.  $k_1[boundEGFR]$
2.  $k_{2f}[EGF][unboundEGFR] - k_{2r}[boundEGFR]$
3.  $\frac{k_3[boundEGFR][inactiveC3G]}{k'_3 + [inactiveC3G]}$
4.  $k_4[activeC3G]$
5.  $\frac{k_5[activeC3G][inactiveRap1]}{k'_5 + [inactiveRap1]}$
6.  $\frac{k_6[activeRap1][BRaf]}{k'_6 + [BRaf]}$
7.  $\frac{k_7[Gap][activeRap1]}{k'_7 + [activeRap1]}$
8.  $\frac{k_8[activeRas][BRaf]}{k'_8 + [BRaf]}$
9.  $\frac{k_9[Gap][activeRas]}{k'_9 + [activeRas]}$
10.  $\frac{k_{10}[activeSOS][inactiveRas]}{k'_{10} + inactiveRas}$
11.  $\frac{k_{11}[activeSOS]}{k'_{11} + [activeSOS]}$
12.  $\frac{k_{12}[boundEGFR][inactiveSOS]}{k'_{12} + [inactiveSOS]}$

### 13.3. Species production rates.

1.  $\dot{[unboundEGFR]} = -k_{2f}[EGF][unboundEGFR] + k_{2r}[boundEGFR]$
2.  $\dot{[inactiveSOS]} = -\frac{k_{12}[boundEGFR][inactiveSOS]}{k'_{12} + [inactiveSOS]} + \frac{k_{11}[activeSOS]}{k'_{11} + [activeSOS]}$

3.  $\dot{[inactiveRas]} = -\frac{k_{10}[activeSOS][inactiveRas]}{k'_{10} + [inactiveRas]} + \frac{k_9[Gap][activeRas]}{k'_9 + [activeRas]}$
4.  $\dot{[inactiveRap1]} = \frac{k_7[Gap][activeRap1]}{k'_7 + [activeRap1]} - \frac{k_5[activeC3G][inactiveRap1]}{k'_5 + [inactiveRap1]}$
5.  $\dot{[boundEGFR]} = k_{2f}[EGF][unboundEGFR] - k_{2r}[boundEGFR] - k_1[boundEGFR]$
6.  $\dot{[activeSOS]} = \frac{k_{12}[boundEGFR][inactiveSOS]}{k'_{12} + [inactiveSOS]} - \frac{k_{11}[activeSOS]}{k'_{11} + [activeSOS]}$
7.  $\dot{[activeRas]} = \frac{k_{10}[activeSOS][inactiveRas]}{k'_{10} + [inactiveRas]} - \frac{k_9[Gap][activeRas]}{k'_9 + [activeRas]}$
8.  $\dot{[activeRap1]} = \frac{k_7[Gap][activeRap1]}{k'_7 + [activeRap1]} + \frac{k_5[activeC3G][inactiveRap1]}{k'_5 + [inactiveRap1]}$
9.  $\dot{[EGF]} = -k_{2f}[EGF][unboundEGFR] + k_{2r}[boundEGFR]$
10.  $\dot{[BRafPP]} = \frac{k_6[activeRap1][BRaf]}{k'_6 + [BRaf]} + \frac{k_8[activeRas][BRaf]}{k'_8 + [BRaf]}$
11.  $\dot{[BRaf]} = -\frac{k_6[activeRap1][BRaf]}{k'_6 + [BRaf]} - \frac{k_8[activeRas][BRaf]}{k'_8 + [BRaf]}$
12.  $\dot{[activeC3G]} = \frac{k_3[boundEGFR][inactiveC3G]}{k'_3 + [inactiveC3G]} - k_4[activeC3G]$
13.  $\dot{[inactiveC3G]} = -\frac{k_3[boundEGFR][inactiveC3G]}{k'_3 + [inactiveC3G]} + k_4[activeC3G]$
14.  $\dot{[degradedEGFR]} = k_1[boundEGFR]$
15.  $\dot{[Gap]} = 0$

**13.4. Initial species concentrations.** All simulations using the above reactions are performed with the following initial concentrations:

1.  $[unboundEGFR]_0 = 500$
2.  $[inactiveSOS]_0 = 1200$
3.  $[inactiveRas]_0 = 1200$
4.  $[inactiveRap1]_0 = 1200$
5.  $[boundEGFR]_0 = 0$
6.  $[activeSOS]_0 = 0$
7.  $[activeRas]_0 = 0$
8.  $[activeRap1]_0 = 0$
9.  $[EGF]_0 = 1000$
10.  $[BRafPP]_0 = 0$
11.  $[BRaf]_0 = 1500$
12.  $[activeC3G]_0 = 0$
13.  $[inactiveC3G]_0 = 1200$

14.  $[degradedEGFR]_0 = 0$
15.  $[Gap]_0 = 2400$

## REFERENCES

- [1] F. Al-Awadhi, M. A. Hurn, and C. Jennison. Improving the acceptance rate of the reversible jump MCMC proposals. *Statistics and Probability Letters*, 69:189–198, 2004.
- [2] S. P. Brooks, P. Giudici, and G. O. Roberts. Efficient construction of reversible jump Markov chain Monte Carlo proposal distributions (with discussion). *Journal of Royal Statistical Society B*, 65:3–39, 2003.
- [3] R. S. Ehlers and S. P. Brooks. Adaptive proposal construction for reversible jump MCMC. *Scandinavian Journal of Statistics*, 35:677–690, 2008.
- [4] Y. Fan, G. W. Peters, and S. A. Sisson. Automating and evaluating reversible jump MCMC proposal distributions. *Statistics and Computing*, 19:409–421, 2009.
- [5] S. J. Godsill. On the relationship between Markov chain Monte Carlo methods for model uncertainty. *Journal of Computational and Graphical Statistics*, 10(2):230–248, 2001.
- [6] P. J. Green. Trans-dimensional Markov chain Monte Carlo. In P. J. Green, N. L. Hjort, and S. Richardson, editors, *Highly Structured Stochastic Systems*. Oxford University Press, Oxford, 2003.
- [7] P. J. Green and A. Mira. Delayed rejection in reversible jump Metropolis-Hastings. *Biometrika*, 88:1035–1053, 2001.
- [8] A. C. Hindmarsh, P. N. Brown, K. E. Grant, S. L. Lee, R. Serban, D. E. Shumaker, and C. S. Woodward. Sundials: Suite of nonlinear and differential/algebraic equation solvers, 2005.
- [9] G. Lawler and A. Sokal. Bounds on the  $L^2$  spectrum for Markov chains and Markov processes. *Transactions of the American Mathematical Society*, 309:557–580, 1988.
- [10] J. D. Murray. *Mathematical Biology: I. An Introduction*. Springer, 3rd edition, 2002.
- [11] T.-R. Xu, V. Vyshevsky, A. Gormand, A. von Kriegsheim, M. Girolami, G. S. Baillie, D. Ketley, A. J. Dunlop, G. Milligan, M. D. Houslay, and W. Kolch. Inferring signaling pathway topologies from multiple perturbation measurements of specific biochemical species. *Science Signaling*, 3(113):ra20, 2010.